AMERICAN PSYCHOLOGICAL ASSOCIATION

Psychological Methods

© 2021 American Psychological Association
ISSN: 1082-989X

2021, Vol. 26, No. 6, 701–718
https://doi.org/10.1037/met0000398

Optimal Sampling Rates for Reliable Continuous-Time First-Order Autoregressive and Vector Autoregressive Modeling

Janne K. Adolf, Tim Loossens, Francis Tuerlinckx, and Eva Ceulemans
Research Group of Quantitative Psychology and Individual Differences, Faculty of Psychology and Educational Sciences, KU Leuven

Abstract

Autoregressive and vector autoregressive models are a driving force in current psychological research. In affect research they are, for instance, frequently used to formalize affective processes and estimate affective dynamics. Discrete-time model variants are most commonly used, but continuous-time formulations are gaining popularity, because they can handle data from longitudinal studies in which the sampling rate varies within the study period, and yield results that can be compared across data sets from studies with different sampling rates. However, whether and how the sampling rate affects the quality with which such continuous-time models can be estimated, has largely been ignored in the literature. In the present article, we show how the sampling rate affects the estimation reliability (i.e., the standard errors of the parameter estimators, with smaller values indicating higher reliability) of continuous-time autoregressive and vector autoregressive models. Moreover, we determine which sampling rates are optimal in the sense that they lead to standard errors of minimal size (subject to the assumption that the models are correct). Our results are based on the theories of optimal design and maximum likelihood estimation. We illustrate them making use of data from the COGITO Study. We formulate recommendations for study planning, and elaborate on strengths and limitations of our approach.

Translational Abstract

Autoregressive and vector autoregressive models are a driving force in current psychological research. In affect research they are, for instance, frequently used to describe affective processes and how these evolve over time. Model variants that estimate processes over discrete time points are most commonly used, but continuous-time formulations are gaining popularity. They allow to handle data from longitudinal studies in which participants were assessed at irregular intervals, and to compare results across data sets obtained at different sampling rates. However, continuous-time models are still estimated from data sampled at discrete time points. Whether and how the data's sampling rate affects how well such continuous-time models can be estimated, has largely been ignored in the literature. In the present article, we show how the sampling rate affects the estimation reliability (i.e., the standard errors of the parameter estimators, with smaller values indicating higher reliability) of continuous-time autoregressive and vector autoregressive models. Moreover, we determine which sampling rates are optimal for estimating the models, in the sense that they

This document is copyrighted by the American Psychological Association or one of its allied publishers.
This article is intended solely for the personal use of the individual user and is not to be disseminated broadly.

This article was published Online First June 24, 2021.
Janne K. Adolf https://orcid.org/0000-0001-6064-9803
Tim Loossens https://orcid.org/0000-0002-7587-1922
Francis Tuerlinckx https://orcid.org/0000-0002-1775-7654
Eva Ceulemans https://orcid.org/0000-0002-7611-4683

The research presented in this article was supported by a short-term postdoctoral stipend from the German Academic Exchange Service (DAAD) and a research fellowship from the German Research Foundation (DFG, Project AD 637/1-1) both awarded to Janne K. Adolf, and by research grants from the Fund for Scientific Research-Flanders (FWO, Project G.074319N) awarded to Eva Ceulemans and from the Research Council of KU Leuven (C14/19/054) awarded to Francis Tuerlinckx and Eva Ceulemans.

This article uses data from the COGITO Study. The principal investigators of the COGITO Study are Ulman Lindenberger, Martin Lövdén, and Florian Schmiedek. Data collection was facilitated by a grant from the Innovation Fund of the President of the Max Planck Society to Ulman Lindenberger.

Early drafts of this article were presented at the International Meeting of the Psychometric Society 2018 in New York, New York, United States, and at the DAGStat Conference 2019 in Munich, Germany.

We thank Michael Hunter for pointing us to Harvey's state space modeling-based formulation of the Fisher information matrix, which proved very useful during the revision of the article.

Correspondence concerning this article should be addressed to Janne K. Adolf, Research Group of Quantitative Psychology and Individual Differences, Faculty of Psychology and Educational Sciences, KU Leuven, Tiensestraat 102, P.O. Box 3713, 3000 Leuven, Belgium. Email: janne.adolf@kuleuven.be

lead to standard errors of minimal size. We illustrate our results with real data from the COGITO Study. We make recommendations for study planning, and elaborate on strengths and limitations of our approach.

Keywords: continuous time first-order vector autoregressive modeling, estimation reliability, maximum likelihood estimation, sampling rate, optimal design

Supplemental materials: https://doi.org/10.1037/met0000398.supp

This document is copyrighted by the American Psychological Association or one of its allied publishers.
This article is intended solely for the personal use of the individual user and is not to be disseminated broadly.

Dynamic models have become popular in psychological research to formalize processes in which present process states depend on past ones (Hamaker & Dolan, 2009). A prominent field of application is affect research, where a new dynamic paradigm (e.g., Hamaker & Wichers, 2017; Kuppens & Verduyn, 2015) conceptualizes affective phenomena as within-person processes and relies on longitudinal studies with intensive assessments of individuals' affective states to capture them. Autoregressive (AR) and vector autoregressive (VAR) models are dynamic models commonly used to unravel how affective processes evolve over time (Bringmann et al., 2016; Hamaker et al., 2015; Kuppens & Verduyn, 2015).

Important insights were obtained with first-order model variants (i.e., AR(1) and VAR(1)), where first-order means that process states at *time t* are predicted on the basis of process states at *time t-1*. For instance, emotions seem to have a tendency to linger on beyond eliciting events (emotional inertia; Kuppens et al., 2010), which is commonly measured via AR parameters in AR(1) or VAR(1) models (De Haan-Rietdijk et al., 2016; Kuppens & Verduyn, 2015; Schuurman et al., 2015); as well as tendencies to *augment* or *blunt* one another. These latter tendencies are usually measured via cross-regressive (CR) parameters in VAR(1) models (Pe & Kuppens, 2012).

Unfortunately, such dynamic approaches to psychological phenomena are not without complications, and recent review papers (Bolger et al., 2003; Hamaker et al., 2015; Hamaker & Wichers, 2017; Trull et al., 2015) have pointed out corresponding research challenges. One of these challenges concerns the sampling rate (SR) that one should use when collecting intensive longitudinal data. Trull and colleagues, for example, note that ". . . assessments should occur at a timescale that is appropriate to the affective processes of interest . . ." (Trull et al., 2015, p. 356). But what is such an appropriate timescale? The literature remains vague on this issue, providing either heuristic answers (for example, "sampling affect at the highest possible frequency . . . may be advisable"; Trull et al., 2015, p. 356) or pointing to the complexity of the problem that therefore requires "careful consideration, theory and empirical studies" (Hamaker et al., 2015, p. 5).

While the problem certainly is complex, it can still be addressed in a principled way. We argue that taking a statistical angle is especially fruitful, in which SRs are derived that are optimal for estimating commonly applied dynamic models. In this paper, we therefore focus on optimal SRs for *continuous-time* (CT) AR(1) and VAR(1) modeling (e.g., Boker, 2012; Oud & Delsing, 2010; Ryan et al., 2018; Voelkle et al., 2012). In CT models, processes are assumed to change continuously in time (Boker, 2002; Driver & Voelkle, 2018b; Karch, 2016). This is in contrast with discrete time (DT) models, in which processes are formulated over discrete observations in time without making assumptions about what happens between subsequent observations.

Elsewhere, authors have emphasized that CT models allow to readily handle missing data and/or unequal SRs within and between studies, which can otherwise cause bias or limit the comparability of results (e.g., Driver et al., 2017; Oud & Delsing, 2010; Voelkle et al., 2012). Here, we focus on them because their account of psychological processes as being continuously ongoing offer a natural context for investigating optimal SRs with optimal sampling intervals (SIs): Obviously, a process cannot be observed continuously in time, but only at discrete measurement occasions. The basic question then becomes when to take these measurements for CT modeling to work out well. While it seems intuitive that we should sample more often from a rapidly changing process in order to not miss out on ongoing fluctuations, does this in fact also lead to modeling solutions of higher quality? And can we slow down the SR for a slowly varying process to reduce participant burden and still get meaningful results? To address these questions, and to formulate recommendations for study planning, we rely on optimal design (OD) theory (Pronzato, 2008) and maximum likelihood (ML) estimation theory.

OD theory deals with the optimality of study design decisions for statistical analysis of the study-generated data. A basic and traditional field of application is (optimal) parameter estimation, with estimation reliability being an often-used optimality criterion. The central question then becomes whether a study design produces data that contain sufficient information to enable reliable estimation of the parameters of interest. In the present article, we will focus on SR decisions in intensive longitudinal studies and their effect on the reliability of CT AR(1) and VAR(1) parameter estimation.

Estimation reliability concerns the estimation or sampling variance of parameter estimators[1], which is commonly reported in terms of standard errors (*SE*s). Smaller *SE*s thereby indicate higher reliability. This form of reliability is also referred to as the precision of parameter estimators. In addition, (higher) distinguishability between different model parameters (i.e., a (smaller) correlation between parameter estimators) is another form of (higher) estimation reliability. Estimation reliability is directly relevant for model-based inference and interpretability. This matters

[1] Note that, throughout the article, we are concerned with estimators and their behavior. To keep this in mind, it might be helpful to think of a theoretical scenario where one keeps drawing different random samples from the population and re-estimates a given model. The behavior of the model's parameter estimators then manifests across the (infinitely) many obtained estimates, as properties of their distribution, also called the sampling distribution. For instance, the variance of this distribution reflects the sampling variance of the estimator, the standard deviation the *SE*. Large *SE*s then point to imprecise point estimators, which are considerably affected by sampling error and are thus unreliable in the sense that they yield results that will less likely reproduce in a different random sample.

This document is copyrighted by the American Psychological Association or one of its allied publishers.
This article is intended solely for the personal use of the individual user and is not to be disseminated broadly.

for CT (V)AR(1) models, which, in the affect domain, often are interpreted literally, as psychological process models. Estimation reliability also has implications for statistical power (Brandmaier et al., 2018; Liu, 2012); and the generalizability of results to unseen data (Bulteel et al., 2018; Vanlier et al., 2012).

To measure estimation reliability, we draw upon ML estimation theory and use the (inverted) Fisher information (FI; Ly et al., 2017). In our case of multiple model parameters, the inverted FI takes the form of a covariance matrix with the estimators' variances in the diagonal and estimators' covariances in the off-diagonal positions. The estimators' *SE*s and correlations can then easily be derived from these variances and covariances. We capitalize on existing results for DT VAR(1) models (Harvey, 1989) to derive an expression for the (inverted) FI of the CT AR(1) and VAR(1) model that can be used to determine reliability-optimal SIs.

To summarize, the present article has a twofold objective: First, we aim to establish how the SR of intensive longitudinal data influences the reliability of parameter estimators of CT AR (1) and VAR(1) models. Second, based on these results, we want to find out whether there are optimal SRs in the sense that they lead to maximally reliable modeling solutions, and how such optimal SRs can be obtained. With this second objective, we obviously aim to prospectively inform design decisions and optimize study planning, rather than to retrospectively measure the impact of past design decisions. We thereby address three problems: Optimizing SRs for reliable estimation of, first, the drift effect in the univariate model, second, a set of multiple drift effects in the univariate model, and, third, the drift matrix in a bivariate VAR model. For the first optimization problem we provide an analytical solution, for the latter two numerical solutions with corresponding *R* functions. We confine the article to SRs with SIs that are constant over time, resulting in equally spaced observations.

The structure is as follows. In the upcoming section The Continuous-Time First-Order Autoregressive and Vector Autoregressive Model, we recapitulate the CT AR(1) and VAR(1) model, their interpretation, and their estimation via the ML method. This section is rather elaborate in order to provide a solid basis for the remainder of the article. In the section Estimation Reliability of the Here-Considered Models and the Role of the Sampling Rate, we give an overview over our reliability derivations and address our first research objective by revealing the role of the SR. The Optimal Sampling Rates section features optimal SRs for the considered models and above scenarios, and thus addresses our second objective. The Discussion section closes the article with a discussion on strengths and limitations of the approach taken, and outlines future directions.

Throughout the article, we complement our arguments and results with illustrations using empirical data from the COGITO Study (Cognition Ergodicity Study of the Max Planck Institute for Human Development; Schmiedek et al., 2010). The COGITO Study is a comprehensive study comprising an intensive longitudinal core that tracked the cognitive and affective development of 101 younger and 103 older adults over, on average, 101 laboratory sessions and 158 days. The daily sessions were in large parts devoted to a broad range of cognitive tasks, but participants also reported affective experiences, which we will focus on here.

The Continuous-Time First-Order Autoregressive and Vector Autoregressive Model

Model Formulation

The Univariate Model

A CT AR(1) model, also known as an *Ornstein-Uhlenbeck* process (Oravecz et al., 2011), can be represented as the first-order stochastic differential equation

$$dy_t = \alpha(y_t - \mu_y)dt + \gamma dW_t, \tag{1}$$

where t denotes time, $\{y_t;\ t \in \mathbb{R}^+\}$ is the process of interest, and dy_t denotes instantaneous change in the process of interest at time t. This change depends on the current process state y_t in deviation from the process mean μ_y and on a CT stochastic error process at time t, $\{dW_t;\ t \in \mathbb{R}^+\}$, which is driven by a standard Wiener process, $\{W_t;\ t \in \mathbb{R}^+\}$, and perturbs the process of interest continuously. The impact of the current process state on the change is scaled by the strictly negative parameter α, and the impact of the CT error process is scaled by the strictly positive parameter γ.

The term $\alpha(y_t - \mu_y)dt$ is called the drift of the process, and governs its expected or average instantaneous change—actual changes are random because of the continuous perturbations from the CT stochastic error process. Because α is negative, the process drift becomes negative, if the process is above its mean, and positive, if it is below its mean. The parameter α is therefore referred to as the drift or mean reversion effect, and the model as stable. The larger the value of the drift effect, the faster the process reverts toward its mean and the lower the autostability; the smaller its value, the longer the perturbations by the error process last and the higher the autostability (cf. Hamilton, 1994). In addition, the rate at which the process of interest drifts also depends on its current value. That is, given a drift effect of a certain size, the process drift is stronger the further the process of interest is away from its mean. The mean-reversion therefore follows an exponential decay-shape. The squared parameter γ^2 is usually referred to as the diffusion effect, because it represents the variance of the scaled CT error process, γdW_t.

The above stochastic differential equation describes instantaneous process change at time t. However, this differential equation can be integrated over a time interval of length Δt, from time $t - \Delta t$ to time t, yielding equation

$$(y_t - \mu_y) = e^{\alpha\Delta t}(y_{t-\Delta t} - \mu_y) + w_{\Delta t,} \tag{2}$$

which now informs us how y_t and $y_{t-\Delta t}$ are related to each other (for a derivation see, e.g., Singer, 2012). The new term $w_{\Delta t}$ denotes the scaled stochastic error process now accumulated over the time interval $[t - \Delta t, t]$ (cf. Appendix C in Voelkle et al., 2012), which follows a Gaussian white-noise process with zero mean and variance $\sigma^2_\varepsilon = \gamma^2(e^{2\alpha\Delta t} - 1)/(2\alpha)$. From this error variance, we can derive the long-run, overall variance of the process by letting Δt increase to infinity. As a consequence—also remember that α is strictly negative—the term $e^{2\alpha\Delta t}$ goes to zero and the variance of y_t becomes $\sigma^2_y = -\frac{\gamma^2}{2\alpha}$.

This document is copyrighted by the American Psychological Association or one of its allied publishers.
This article is intended solely for the personal use of the individual user and is not to be disseminated broadly.

This reformulation of the model makes the relation between the CT and the well-known DT AR(1) model evident (e.g., Equation 4 in Ryan et al., 2018): For a time interval of length $\Delta t = s$, the model implies a DT AR(1) effect of size $\phi(s) = e^{\alpha s}$.[2] Keeping this link in mind can be useful to interpret CT drift effects and we will make use of this in the following. Also, we consider the case where the process of interest fluctuates around a zero mean (i.e., $\mu_y = 0$), which is without loss of generality for our results.[3]

The Multivariate Model

The multivariate model extends the just-described dynamic equations to multiple processes. The first-order stochastic differential equation underlying the CT VAR(1) model thus equals

$$d\mathbf{y}_t = \mathbf{A}(\mathbf{y}_t - \boldsymbol{\mu}_y)dt + \boldsymbol{\Gamma} d\mathbf{W}_t \tag{3}$$

and features a $p \times 1$ *vector* of processes of interest, $\{\mathbf{y}_t;\ t \in \mathbb{R}^+\}$, a $p \times 1$ *vector* of corresponding process means, $\boldsymbol{\mu}_y$, and a $p \times 1$ *vector* of CT stochastic error processes, $\{d\mathbf{W}_t;\ t \in \mathbb{R}^+\}$, consisting of instantaneous change in p independent standard Wiener processes, $\{\mathbf{W}_t;\ t \in \mathbb{R}^+\}$. Modeling multiple processes simultaneously allows to capture that processes might not only be related to themselves, but also to each other. So, instead of a single drift effect α we have a $p \times p$ *matrix* of drift effects denoted by $\mathbf{A}$, which contains the CT AR effects that processes exert on themselves over time on the main diagonal and the CT CR effects that processes exert on each other over time on the off-diagonal positions. Also, the CT error processes affect the processes of interest via a $p \times p$ *matrix* $\boldsymbol{\Gamma}$. Whereas a diagonal element of $\boldsymbol{\Gamma}$ scales the impact of a CT error process on the corresponding process of interest, an off-diagonal element allows a CT error process to have an additional effect on another processes of interest and can hence account for correlated process errors. Stable, mean-reverting processes are guaranteed if the real parts of all eigenvalues of the drift matrix $\mathbf{A}$ are negative (Oud & Delsing, 2010; Voelkle et al., 2012). For these cases, the CT AR effects on the main diagonal will often be negative too, but need not strictly be, depending on the CT CR effects. The $p \times p$ matrix $\boldsymbol{\Gamma}\boldsymbol{\Gamma}'$, with $\boldsymbol{\Gamma}'$ being the transpose of $\boldsymbol{\Gamma}$, is referred to as the diffusion matrix and represents the covariance matrix of the CT error processes.

After integrating over a time interval Δt, the CT VAR(1) model can be written as

$$(\mathbf{y}_t - \boldsymbol{\mu}_y) = e^{\mathbf{A}\,\Delta t}(\mathbf{y}_{t-\Delta t} - \boldsymbol{\mu}_y) + \mathbf{w}_{\Delta t} \tag{4}$$

where $\mathbf{w}_{\Delta t}$ is a $p \times 1$ vector of Gaussian white-noise processes with zero mean and $p \times p$ covariance matrix $\boldsymbol{\Sigma}_\varepsilon$, which can be written in vectorized from (i.e., stacked by column) as $vec(\boldsymbol{\Sigma}_\varepsilon) = (\mathbf{A} \otimes \mathbf{I} + \mathbf{I} \otimes \mathbf{A})^{-1}\ (e^{(\mathbf{A}\otimes\mathbf{I}+\mathbf{I}\otimes\mathbf{A})\,\Delta t} - \mathbf{I} \otimes \mathbf{I})\ vec(\boldsymbol{\Gamma}\boldsymbol{\Gamma}')$, with $\mathbf{I}$ being a $p \times p$ identity matrix. If we let Δt go to infinity, the term $e^{(\mathbf{A}\otimes\mathbf{I}+\mathbf{I}\otimes\mathbf{A})\,\Delta t}$ goes to zero[4], and we obtain the vectorized long-run variance of the process $\mathbf{y}_t$ as $vec(\boldsymbol{\Sigma}_y) = (\mathbf{A} \otimes \mathbf{I} + \mathbf{I} \otimes \mathbf{A})^{-1}\ (-\mathbf{I} \otimes \mathbf{I})\ vec(\boldsymbol{\Gamma}\boldsymbol{\Gamma}')$.

Again, for a given SI $\Delta t = s$, the model implies a matrix of DT AR and CR effects of the form $\boldsymbol{\Phi}(s) = e^{\mathbf{A}\,s}$. It is important to note that, in contrast to the univariate model, the exponential function here is a *matrix* exponential function. The implied DT AR and CR effects are thus complicated nonlinear functions of all CT AR and CR effects and the SI, which means that the model's dynamic behavior cannot as easily be deduced from the CT drift matrix as for the univariate model. We will however provide an illustrative example in the following section.

As for the univariate model, we assume that the processes of interest fluctuate around zero means (i.e., $\boldsymbol{\mu}_y = \mathbf{0}$). Also, we only consider models with drift matrices that have purely real-valued eigenvalues. Drift matrices with complex eigenvalues imply oscillatory processes (see e.g., Voelkle & Oud, 2013); which behave differently (Boker, 2012; Chow et al., 2005) and are also not often applied to psychological data.

Illustration With COGITO Data

To illustrate the CT AR(1) and VAR(1) model, we present some first COGITO results. For the following analyses—all performed in *R* (v3.6.1; R Core Team, 2017)—we considered the subsample of the younger participants (N = 101; 51.5% women; age: 20–31, M = 25.6; daily sessions: 87–109, M = 101; days in study: 116–372, M = 165) and their daily reports of negative affect (NA) and positive affect (PA) as assessed by a German version of the Positive and Negative Affect Schedule (Watson et al., 1988). This instrument consists of 10 PA and 10 NA items. Participants used an 8-point scale to respond to the items, with response categories ranging from 0 (*does not apply at all*) to 7 (*applies very well*).

Before fitting the models to participants' affect time series, we took two preprocessing steps. First, to render the data more continuous and potentially normal, we calculated average scores across all 10 PA and across the five most variable NA items (i.e., *distressed, upset, irritable, nervous, jittery*). Excluding the remaining items constitutes a common strategy to deal with low variability in the NA data of the COGITO Study (e.g., Brose et al., 2012). Second, we removed potential mean trends from the data, which are not handled by the discussed models, by regressing the averaged time series on days in study via local polynomial regression (Cleveland et al., 1993); as implemented in the *R*-base function *loess*. We used a smoothing span of .5 following earlier applications of local polynomial regression to preprocess the COGITO data (Voelkle et al., 2014). To estimate the CT AR(1) and VAR(1)

[2] Note that the unit of time, specifically, the unit of the SI Δt over which we integrate, is not defined. In psychological applications, this unit could be a second, an hour, or a day, depending on the type of data to be modeled (e.g., physiological measures, self-report). For a given time interval, the size of Δt varies depending on the unit of time used (Δt_{sec} = 60 versus Δt_{min} = 1). Because Δt is multiplied with the drift effect in the above equation, α and Δt become exchangeable, and α also varies depending on the unit of time (cf. Kuiper & Ryan, 2018). Of course, in which unit a given time interval is measured is arbitrary, and does not affect our general results. But it should be taken into consideration when interpreting the sizes of CT effects, and corresponding optimal SRs, as we will show in the following.

[3] At least, if a non-zero mean would be estimated independent of the recursive part of the model, for instance, as the intercept in a measurement model.

[4] This is due to the negative real parts of the eigenvalues of $\mathbf{A}$, which can be seen from the eigenvalue-based representation of the matrix exponential presented in Equation 10 of the online supplementary material.

This document is copyrighted by the American Psychological Association or one of its allied publishers.
This article is intended solely for the personal use of the individual user and is not to be disseminated broadly.

models, we rely on our own implementation[5] via the *R*-package *OpenMx* (*v2.17.4*; Neale et al., 2016) and its state space modeling functionality (Hunter, 2018). A modeling script can be found in Section 3.1 in the online supplementary material.

To render the illustration coherent and easy to follow throughout the article, we decided to limit the number of presented modeling solutions. Specifically, we included younger COGITO participants only if all their solutions were free from critical optimization errors (status codes >1 as reported by *OpenMx*). Next, their data had to yield stable univariate solutions for both NA and PA, and stable, nonoscillating multivariate solutions for NA and PA. Finally, we excluded a few participants whose multivariate solutions implied negative DT AR effects, because such effects are hardly interpretable in psychological applications. Although the employed listwise deletion is restrictive, it has the advantage that the illustration results are comparable throughout the article in that they are all based on the same set of participants. In any case, our focus lies not so much on individual modeling solutions and their interpretation, but rather on a principled illustration of model-based SR optimization. Table 2 in Section 4.1 of the online supplementary material provides an overview of the excluded cases and the exclusion criteria they meet. It reveals that for around half of the excluded participants at least one of their (mostly VAR) modeling solutions yielded optimization errors—we elaborate on potential reasons in the online supplementary material—and around a third of the exclusions are due to complex eigenvalues of the CT VAR drift matrix indicating oscillatory behavior.

Moving from the excluded to the included cases, Table 3 in Section 4.2 of the online supplementary material summarizes all 33×3 modeling solutions presented in the article, and Figure 1 provides an exemplary display of one selected participant. Panel A reveals their modeled affect time series, Panels B and C depict path diagrams of the fitted models, and Panels D and E the model-implied impulse response functions, visualizing the models' dynamic behavior.[6]

First, considering the univariate modeling solutions (Panel B in Figure 1), the selected participant is exemplary in that we estimate a relatively high autostability for NA, $\hat{\alpha}_{1obs} = -0.58$, implying a DT AR effect across days of $\hat{\phi}(1)_{1obs} = 0.56$ (solid red lines in all panels of Figure 1), and a relatively low autostability for PA, $\hat{\alpha}_{2obs} = -1.43$, corresponding to a DT AR effect across days of $\hat{\phi}(1)_{2obs} = 0.24$ (dashed blue lines in all panels of Figure 1). Panel A demonstrates these different temporal structures at the level of the data: While there are substantial carry-over effects between adjacent days in the solid red trajectory, this temporal pattern is less evident for the dashed blue trajectory, which fluctuates in a less structured manner over time. The impulse response functions of the two CT AR(1) models (Panel D) illustrate these differences more clearly. In principle, they visualize the models' behavior under controlled conditions, that is, the processes of interest's reaction to a single controlled impulse (i.e., a realization of the stochastic error process of value one, assuming that the process of interest had assumed its mean value a priori; Lütkepohl, 2005). In the resulting trajectories—which are also a visualization of the exponential function featuring in the first (deterministic) part of Equation 2 and thus display the implied DT AR effects over time intervals—we can see how the effect of the impulse would diminish or "die out" (Hamilton, 1994, p. 54) over time, and hence how quickly the processes would return to their means were there no further perturbations. As explained in the section The Univariate Model, this return is scaled by the drift effect in that larger values imply a faster return (dashed blue line) than smaller values closer to zero (solid red line).

Considering the multivariate modeling solution (Panel C), we note that NA remains relatively autostable ($\hat{\alpha}_{11obs} = -0.86$, corresponding to a DT AR effect of size $\hat{\phi}(1)_{11obs} = 0.52$ across days) even after controlling for PA, which exerts a negative CR effect on NA ($\hat{\alpha}_{12obs} = -1.20$, corresponding to a DT CR effect of $\hat{\phi}(1)_{12obs} = -0.29$ across days), and seems to show some contemporaneous overlap with NA. PA itself is much less autostable ($\hat{\alpha}_{22obs} = -2.42$, corresponding to a DT AR effect of $\hat{\phi}(1)_{22obs} = 0.15$ across days), and also affected by NA via an also negative, but smaller CR effect ($\hat{\alpha}_{21obs} = -0.57$, corresponding to a DT CR effect of $\hat{\phi}(1)_{21obs} = -0.14$ across days). Note that the two CR effects are not standardized, so in comparing them, we do not control for possible differences in the amount of variation between the two processes here. The negative interaction between the two processes is visible in the data (again Panel A of Figure 1), in the sense that the processes seem to consistently mirror each other, albeit in a time-lagged fashion. In Panel E we now see the multivariate model's response to a single controlled impulse that is either administered to NA (left graph in panel) or to PA (right graph in panel). The resulting trajectories display, again, an exponential decay in the case of the processes affecting themselves. In the case of the processes affecting each other, however, the trajectories start at zero at the time of the impulse, peak at a later time, here after approximately .75 days, and then diminish again. An intuitive account of this shape is that it takes time for one process to affect another one (Deboeck & Preacher, 2016). As in the univariate model, CT AR effects of different strength manifest in terms of impulse responses that diminish at different pace. CT CR effects of different strength manifest themselves in terms of impulse responses that peak at different heights. The timing of the peak is invariant across processes in bivariate CT VAR(1) models.

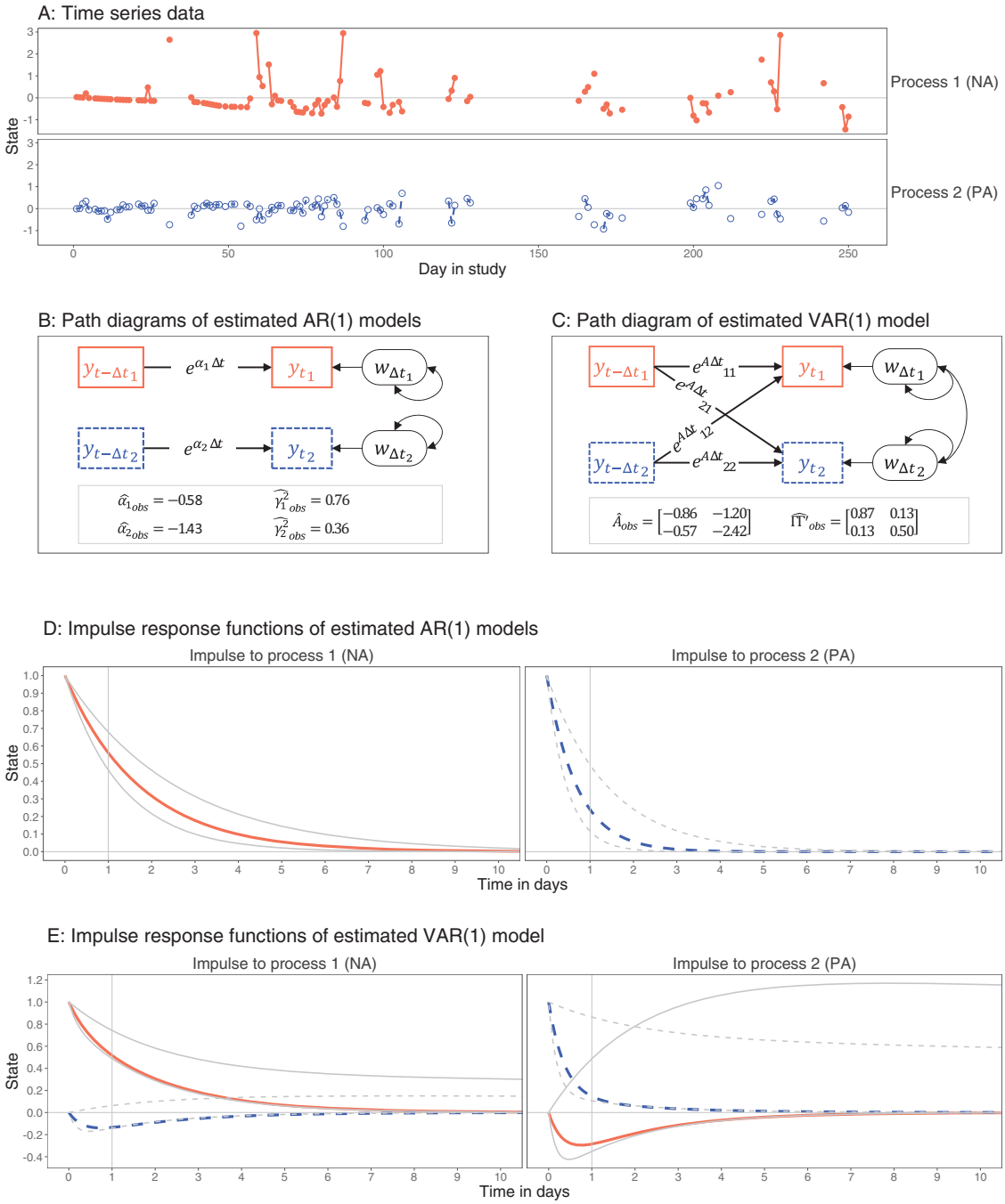
These illustrations of the models pinpoint their substantive attractiveness: If one believes that affective processes are characterized by an equilibrium or preferred state, which they are normally regulated back to, after external or internal events or other affective processes have taken their excitatory effect, then CT (V)AR(1) models are obvious candidates to formalize such ideas (Adolf, 2018; Chow et al., 2005; Kuppens et al., 2010). Regulatory interpretations of the drift effects are a logical consequence and quite common, be it the interpretation of CT AR effects—or their

[5] The advantage of using our own implementation over available ones, mainly *ctsem* (Driver et al., 2017), is that the models are parameterized as described. *ctsem*, on the contrary, uses covert reparameterizations, which aid optimization but come with different FI matrices. Replicating our univariate analyses in *ctsem* reveals that modeling solutions correlate highly in terms of model fit ($r > .99$).

[6] In the figure and afterwards, we employ the so-called *hat notation* to distinguish parameter estimators and estimates from model parameters at the population-level. In addition, we add the subscript *obs* for *observed* if we consider an estimate rather than an estimator. Using the drift effect as an example, α denotes the population-level effect, $\hat{\alpha}$ denotes the estimator as a function of observable data, and $\hat{\alpha}_{obs}$ is the estimate as a function of observed data.

Figure 1

Illustration of the CT AR(1) and VAR(1) Model on Basis of Data From One Participant of the COGITO Study



Note. Panel A shows the smoothed time series data for negative and positive affect, Panels B and C display the estimated models in terms of path diagrams, and Panels D and E show the model-implied impulse response functions. For the impulse response functions, we assume that a single impulse of size 1 at Time 0 drives the process of interest away from its mean and thus leads to an initial process value of one and mean-reverting values afterwards. A gray vertical line marks a time interval of one as a reference. Across all panels, solid red lines identify negative affect or Process 1, and dashed blue lines identify positive affect or Process 2. See the online article for the color version of this figure.

This document is copyrighted by the American Psychological Association or one of its allied publishers.
This article is intended solely for the personal use of the individual user and is not to be disseminated broadly.

DT analogues—as *emotional inertia* or *regulatory weakness* (e.g., Brose et al., 2015; De Haan-Rietdijk et al., 2016; Koval et al., 2015; Kuppens et al., 2010; Suls et al., 1998), or the interpretation of cross drift effects—or their DT analogues—as *emotional augmentation* or *blunting* (Pe & Kuppens, 2012).

Model Estimation

Maximum Likelihood Estimation

We apply ML estimation (Driver et al., 2017; Oud & Delsing, 2010; Singer, 2012; Voelkle et al., 2012). To formulate the log-likelihood function of the CT AR(1) and VAR(1) model, we rely on Equations 2 and 4. These equations express the CT processes in terms of discrete time points and thus allow to map them onto observable DT data. ML estimates of the CT parameters $\boldsymbol{\theta} = \{\alpha_{11}, \alpha_{21}, \alpha_{12}, \alpha_{22}, \gamma\gamma_{11}, \gamma\gamma_{21}, \gamma\gamma_{22}\}$ can then be obtained by maximizing the log-likelihood function typically reported in the VAR modeling literature (cf. Hamilton, 1994; Harvey, 1989):

$$\ell\left(\boldsymbol{\theta}; \mathbf{y}_{t_1}, \mathbf{y}_{t_k}, \ldots, \mathbf{y}_{t_T}\right) = \ell\left(\boldsymbol{\theta}; \mathbf{y}_{t_1}\right) + \sum_{k=2}^{T} \ell\left(\boldsymbol{\theta}; \mathbf{y}_{t_k} | \mathbf{y}_{t_{k-1}}\right). \quad (5)$$

Equation 5 describes the joint log-likelihood function for all time points, t_1 and $\{t_k; k \in 2, 3, \ldots, T\}$, at which the process is to be observed or sampled with SI Δt, with T being the total number of time points, $\mathbf{y}_{t_1}$ being the $p \times 1$ vector of process states at the first time point, and $\mathbf{y}_{t_k}|\mathbf{y}_{t_{k-1}}$ being the $p \times 1$ vector of process states at the k-th time point conditional on the process states at the $(k-1)$-th time point. Note that although this log-likelihood function is formulated for the VAR(1) model, it of course also applies to the AR(1) model with parameters $\boldsymbol{\theta} = \{\alpha, \gamma^2\}$ as a special case.

The joint log-likelihood function thus splits into two terms. The first term, $\ell(\boldsymbol{\theta}; \mathbf{y}_{t_1})$, represents the log-likelihood contribution of the first time point, the second term sums the contributions of the remaining $(T-1)$ time points. For these latter time points, we deal with conditional observations, $\mathbf{y}_{t_k}$ given $\mathbf{y}_{t_{k-1}}$, and assume that they come from the conditional distribution implied by each model. These are normal distributions with mean vector $\boldsymbol{\mu}_{y|\cdot} = e^{\mathbf{A}\Delta t}\mathbf{y}_{t_{k-1}}$ and covariance matrix $\boldsymbol{\Sigma}_{y|\cdot} = \boldsymbol{\Sigma}_{\varepsilon}$ in case of the multivariate model, and mean $\mu_{y|\cdot} = e^{\alpha\Delta t}y_{t_{k-1}}$ and variance $\sigma^2_{y|\cdot} = \sigma^2_{\varepsilon}$ in case of the univariate model. For the first time point, we assume that the observations are drawn from the long-run distribution of each model because we consider stable processes and have no prior observations to condition on. These long-run distributions had zero means and covariance matrix $\boldsymbol{\Sigma}_y$ and variance σ^2_y, respectively. The exact expressions of the log-likelihood terms are given in the online supplementary material (Section 1.2).

ML estimation theory provides a well-established, comprehensive framework for parameter estimation and statistical inference, and estimators are known to have optimal properties (Myung, 2003). Moreover, as mentioned in the introduction, ML estimation theory is especially useful in the present context, since it establishes the inverted FI (Ly et al., 2017) as a theory-based measure of estimation reliability. Specifically, it has been shown that the inverse of the FI reflects the asymptotic sampling (co-)variances of ML parameter estimators.[7] As such, the FI is not only commonly used to generate *SE*s, but also features regularly in OD theory applications (e.g., Dobos & Abonyi, 2013; Eisenberg & Hayashi, 2014; Pronzato, 2008; Shardt & Huang, 2013). In the Discussion section, we elaborate on what it means that we base our results on estimation theory, and thus consider estimation reliability in the asymptotic case, for very large numbers of time points.

Illustration With COGITO Data

We come back to the exemplary COGITO participant. When estimating the models, we obtain the following FI-based *SE*s: $SE_{\hat{\alpha}1} = 0.72$, $SE_{\hat{\alpha}2} = 0.19$, $SE_{\hat{\gamma}^2 1} = 0.17$, $SE_{\hat{\gamma}^2 2} = 0.19$ for the two univariate solutions, and $SE_{\hat{\alpha}_{11}} = 0.54$, $SE_{\hat{\alpha}_{21}} = 0.64$, $SE_{\hat{\alpha}_{12}} = 1.81$, $SE_{\hat{\alpha}_{22}} = 2.25$, $SE_{\hat{\gamma}^2 11} = 0.33$, $SE_{\hat{\gamma}^2 21} = 0.31$, $SE_{\hat{\gamma}^2 22} = 0.44$ for the multivariate solution. For the drift effects, Panels D and E of Figure 1 visualize these estimation unreliabilities by adding to the standard impulse response (thicker colored lines, solid for Process 1, dashed for Process 2), the impulse responses implied by the drift effect estimates one *SE* below and above their ML point estimate (thinner gray lines, solid for Process 1, dashed for Process 2). Apparently, there is quite some uncertainty with respect to the strength of CT AR and CR effects. In the latter case there might even be no reliable CR effects, or CR effects of opposite sign than indicated by the point estimates. Remember that a negative CR effect would be indicative of *emotional blunting* while a positive CR effect would be indicative of *emotional augmentation*, two distinct phenomena (Pe & Kuppens, 2012). This demonstrates how imprecise parameter estimators are uninformative and undermine the interpretation of model parameters in terms of psychological characteristics.

Moreover, we can take a look at parameter distinguishability, for instance for the univariate modeling solutions. Here, we obtain FI-based parameter estimator correlations[8] that are quite large, $COR_{\hat{\alpha}\hat{\gamma}^2 1} = -0.95$ and $COR_{\hat{\alpha}\hat{\gamma}^2 1} = -0.82$. This means that, with little consequences for model fit, we could trade larger (negative) values of α indicating lower autostabilities for larger values of γ^2 indicating higher CT process error variances. The two parameters become to some extent exchangeable. Also this hampers interpretability, given the usually strong substantive interest in the drift or the implied DT AR effects. The consequences of low distinguishability become even more evident, if different parameters are thought to indicate distinct, nonexchangeable psychological parameters (e.g., *emotional inertia* vs. *emotional blunting* or *augmentation*). We briefly return to this case in the following section.

[7] Under certain general and rather technical conditions required for valid ML estimation, for instance that the unknown parameter is in the interior of the parameter space.

[8] *OpenMx* numerically approximates the FI matrix during model estimation. The full matrix is then returned as part of the fit object and can easily be retrieved (cf. Sections 3.2 and 3.3 in the online supplementary material).

This document is copyrighted by the American Psychological Association or one of its allied publishers.
This article is intended solely for the personal use of the individual user and is not to be disseminated broadly.

This document is copyrighted by the American Psychological Association or one of its allied publishers.
This article is intended solely for the personal use of the individual user and is not to be disseminated broadly.

Estimation Reliability of the Here-Considered Models and the Role of the Sampling Rate

Analytical Expressions for the (Inverted) Fisher Information

The FI can in principle be derived from the log-likelihood function of a model (Enders, 2010). In the present case, we rely on an existing derivation: Harvey (1989, p. 142, Equation 3.4.69) provides a general formula for the FI of VAR(1) models. It is derived for DT VAR(1) models, but also applies to CT VAR(1) and AR(1) models when formulated according to Equations 2 and 4. Adapted to our notation and discussed model variants, the expression equals

$$\begin{aligned}\mathcal{I}(\boldsymbol{\theta})_{ij} = &\frac{1}{2} tr\left(\boldsymbol{\Sigma}_y^{-1} \frac{\partial\, \boldsymbol{\Sigma}_y}{\partial \theta_i}\ \boldsymbol{\Sigma}_y^{-1} \frac{\partial\, \boldsymbol{\Sigma}_y}{\partial \theta_j}\right) \\ &+ \frac{T-1}{2}\left(tr\left(\boldsymbol{\Sigma}_{y|\cdot}^{-1} \frac{\partial\, \boldsymbol{\Sigma}_{y|\cdot}}{\partial \theta_i}\ \ \boldsymbol{\Sigma}_{y|\cdot}^{-1} \frac{\partial\, \boldsymbol{\Sigma}_{y|\cdot}}{\partial \theta_j}\right)\right) \\ &+ E\left(\sum_{k=2}^{T}\left(\left(\frac{\partial\, \boldsymbol{\mu}_{y|\cdot}}{\partial \theta_i}\right)' \boldsymbol{\Sigma}_{y|\cdot}^{-1} \frac{\partial\, \boldsymbol{\mu}_{y|\cdot}}{\partial \theta_j}\right)\right), \end{aligned} \tag{6}$$

where $\mathcal{I}(\boldsymbol{\theta})_{ij}$ denotes the entry of the FI matrix $\mathcal{I}(\boldsymbol{\theta})$ concerning the pair of parameters $\{\theta_i, \theta_j\}$. Note that the right-hand side of the equation features the model-implied (un-)conditional (co-)variances and means that we discussed when presenting the log-likelihood function (Equation 5), and remember that these could be expressed as a function of the model parameters. In the online supplementary material (Section 1.3.2), we show in detail how the whole expression can be reformulated until it consists of familiar elements only, namely the model parameters, and the total number of time points, and, importantly, the SI. The resulting formulation can be found in Equation 18 in Section 1.3.3 of the online supplementary material.

For the simpler CT AR(1) model, we can then derive explicit expressions for all elements of the FI-based parameter estimator covariance matrix using *Mathematica* (v.11.3; Wolfram Research, 2018; see Equations 22 to 24 in the online supplementary material, Section 1.4), and in a final step even an explicit expression for optimal SRs (derivation detailed also in the online supplementary material, Section 1.5). For the CT VAR(1) model it does not seem feasible to go that far analytically. However, based on the FI formulation we derive in the online supplementary material, we can easily calculate the (exact) FI matrix and the (exact) FI-based parameter estimator covariance matrix for any sensible population parameter values, total number of time points and SI. Combining that with standard numerical optimization methods enables us to derive optimal SRs also for the multivariate model. Note that our optimization function is currently confined to bivariate model variants, although the derived FI expression is in principle not (cf. Section 1.3.2 in the online supplementary material, p. 9, for more detail).

The Role of the Sampling Rate

To address our first research objective, let us take a look at the how the SR affects estimation reliability. For the univariate model, we include this here, for the multivariate model, we include a section in the online supplementary material (Section 1.6, Figure 2). Here, Figure 2 displays the relationship between the SR as defined by its SI, Δt, and the estimation reliability of the CT AR(1) model parameter estimators. The different forms of estimation reliability, precision and distinguishability, are thereby displayed in different panels. Panels A and B show the precisions of the drift and diffusion effect estimators in terms of their FI-based *SE*s, $SE_{\hat{\alpha}}$ and $SE_{\hat{\gamma}^2}$, and Panel C shows the distinguishability of the estimators in terms of their FI-based correlation, $COR_{\hat{\alpha}\hat{\gamma}^2}$, calculated from the estimators' covariance and *SE*s.

We used our derived reliability expressions (Equations 22 to 24 in the online supplementary material) to generate large parts of the figure, specifically the line plots.[9] These analytical reliabilities are presented conditional on selected population parameter values for the drift and the diffusion effect, and conditional on different total numbers of observations T. Results for different population values of the drift effect α, and thus differentially autostable processes, are distinguished per plot via line-type. Specifically, dashed lines signify a drift effect of $\alpha = \ln(.1) \approx -2.303$, dash-dotted lines a drift effect of $\alpha = \ln(.5) \approx -0.693$, and solid lines a drift effect of $\alpha = \ln(.9) \approx -0.105$, corresponding to small, medium, and very large DT AR effects at a SI of $\Delta t = 1$, respectively. We select these values, which may be more or less plausible for psychological processes, to clearly illustrate the effects of the population drift effect size on the estimation reliability. Results for low versus high population values of the diffusion effect (i.e., $\gamma^2 = .5$, $\gamma^2 = 1.5$) are organized per panel in different rows, whereas results for different numbers of observations are organized in different columns. Note that, in Panel A, we do not condition on the diffusion effect because it does not matter for the FI-based *SE* of the drift effect estimator (i.e., the drift effect is standardized by virtue of the recursive nature of the model, and γ^2 does not appear in the expression for the drift estimator's variance).

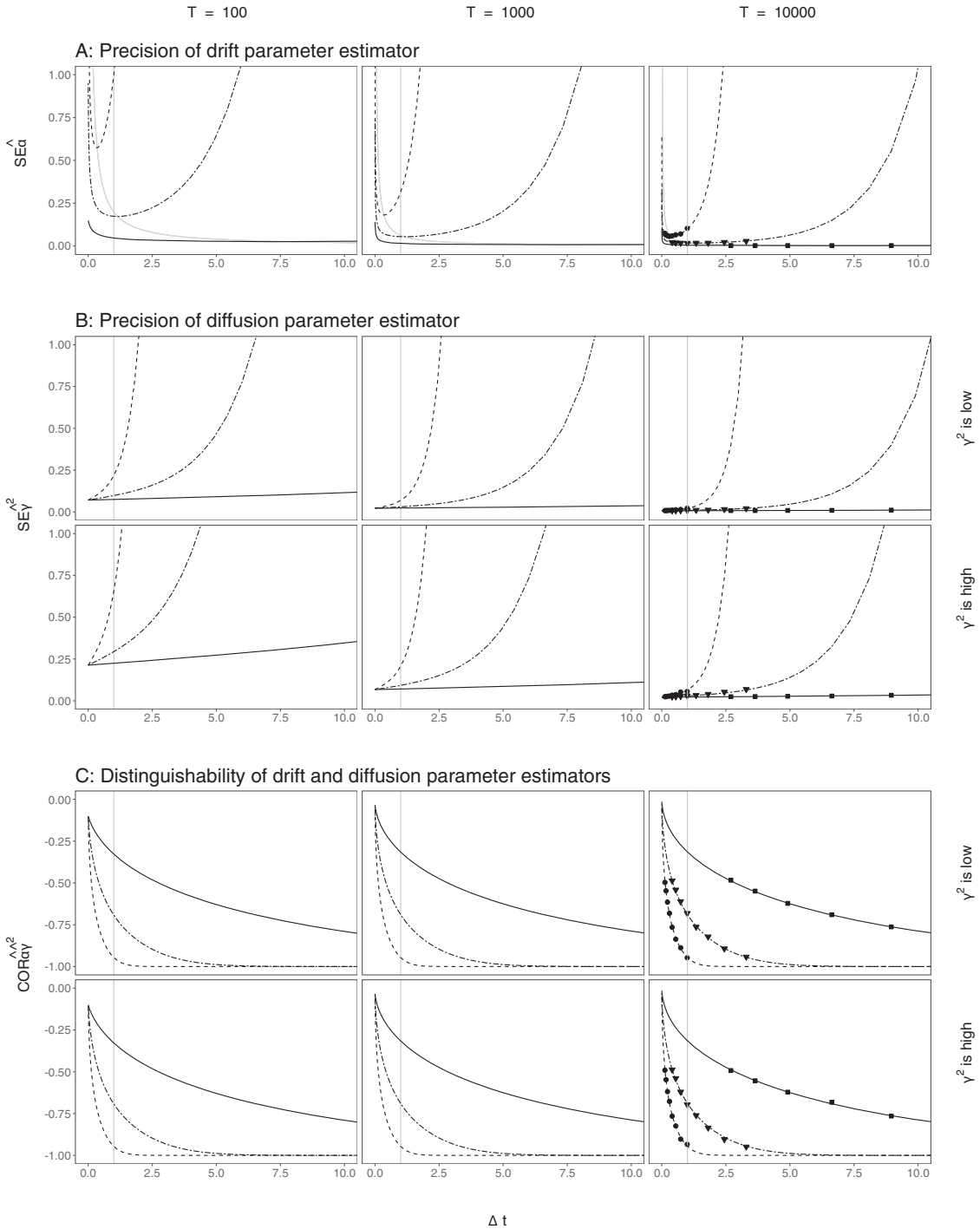
Considering Figure 2 overall, we see that larger SIs (i.e., slower SRs) are associated with reliability losses in terms of decreasing parameter estimator precisions and distinguishability. Also, all remaining factors seem to affect estimation reliability, in that drift effects closer to zero (indicating higher autostability), lower diffusion effects, and larger number of observations all seem to imply higher reliabilities overall.

Furthermore, two patterns of interaction effects are evident. The first is that the magnitude and shape of the reliability losses due to slowing down the SR depend strongly and mainly on the size of α. The higher the value of α (i.e., the lower the autostability), the more severe the reliability losses. This manifests in *SE*s that barely show any change until SIs are around $\Delta t = 10$ if autostabilities are very high, but show steep increases already at SIs around $\Delta t = 2$ if autostabilities are low. It also manifests in a parameter estimator correlation that does not exceed values of $-.75$ until SIs are

[9] In addition to the line plots, there are occasional points. These represent independent empirical results, as they originate from estimated FI matrices obtained through fitting the model in *OpenMx* to time series simulated with the respective parameter values. We add these results only for the longest time series and only for selected SIs to give an idea of the agreement of theory- and simulation-based results under rather ideal conditions, and indeed, for the plotted scenarios, results from both sources seem to align very well.

Figure 2

FI-Based Estimation Reliability for the CT AR(1) Model as a Function of the SR



Note. Panel A displays the precision of the drift estimator in terms of its FI-based *SE*, Panel B the precision of the diffusion estimator in terms of its FI-based *SE*, and Panel C the FI-based correlation between the two parameter estimators indicating their distinguishability. These analytical reliabilities are presented conditional on different population parameter values and total numbers of observations: Dashed lines signify high, dash-dotted lines medium, and solid lines small drift effects, corresponding to low, medium, and high autostabilities, respectively. Results for low and high population values of the diffusion parameter are presented in different rows, and results for different numbers of observations are presented in different columns per panel. Gray vertical lines mark SIs of one as a reference. Points represent empirical reliability results, obtained through fitting the model in OpenMx to data simulated with the respective parameter values. Population drift values are coded by the shape of the points. Results from processes with low autostability are shown as circles, results from medium autostable processes as triangles, and results from highly autostable processes as rectangles.

This document is copyrighted by the American Psychological Association or one of its allied publishers.
This article is intended solely for the personal use of the individual user and is not to be disseminated broadly.

This document is copyrighted by the American Psychological Association or one of its allied publishers.
This article is intended solely for the personal use of the individual user and is not to be disseminated broadly.

around $\Delta t = 7$ if autostabilities are very high, but practically reaches its asymptote of a perfect negative correlation at SIs as small as $\Delta t = 2$ if autostabilities are low. The population parameter value of the diffusion effect and the total number of observations also moderate the SR-related reliability losses (e.g., there is a lowered impact of the SR on the precisions given larger numbers of observations), but these factors clearly matter much less, at least for the values we have conditioned on here.

The second pattern concerns the interaction of the SR and which parameter is estimated, and already hints at the results to our second research objective, determining optimal SRs: Whereas Panel B and C yield monotonically increasing functions (i.e., larger SIs seem always associated with higher imprecision of the diffusion estimator and higher correlations between diffusion and drift estimator), the *SE*-curves presented in Panel A show an initial decrease preceding the later increase. This means that there must be SRs for which the estimator of the drift parameter is maximally reliable. Where these optimal SRs are located seems to—again—foremost depend on the size of the drift effect in the population (i.e., the more autostable the process, the larger the optimal SI).

For the CT VAR(1) model and its parameter estimators, we include visualizations of the FI-based estimation reliabilities in the online supplementary material. The reason is twofold: Due to the higher number of parameters in the multivariate model, there are many more parameter covariance matrix elements (28 instead of three in a bivariate model) and even more combinations of population parameter values to consider. However, to give a brief summary, the multivariate reliability results share the main qualitative characteristics of the univariate results: The strengths of the population-level drift and especially the CT AR effects seem to be major factors in determining how severely increasing SIs impair estimation reliability, when assessed in terms of *SE*s and roughly also in terms of parameter estimator correlations. With respect to the latter, a difference to the univariate case is that certain parameter trade-offs are quite pronounced. Especially those drift effects that feed into the same process (i.e., AR effect α_{11} and CR effect α_{12} or AR effect α_{22} and CR effect α_{21} in Figure 1) can be highly correlated (see Figure 4 in Section 1.6.3 of the online supplementary material). Because the SI does not seem to have much impact on these generally high correlations, it becomes even more important to estimate these drift effects with high precision, so that the trade-off cannot play out as much, and their distinct interpretations can be preserved. Fortunately, also, for the drift effect estimators in the CT VAR(1), there seem to be optimal SIs at which their precision is maximal.

Optimal Sampling Rates

Optimal Sampling Rates for Reliable Drift Effect Estimation in the Univariate Model

Minimizing the Variance of the Drift Effect Estimator

We now turn to our second research objective, determining reliability-optimal SRs. We thereby focus on the drift effects, because for these effects optimal SRs exist, as we have seen in the previous section. Moreover, they are often of high psychological interest. In this section, we start with the drift effect in a CT AR(1) model. The FI-based variance of the drift estimator $\hat{\alpha}$ is displayed in Equation 22 in the online supplementary material, but we recapitulate the expression here:

$$\sigma^2_{\hat{\alpha}} = -\frac{Te^{-2\alpha\Delta t}\left(e^{2\alpha\Delta t}-1\right)^2}{\Delta t^2(T-1)\left((T-2)e^{2\alpha\Delta t}-T\right)} \tag{7}$$

SRs that maximize the reliability with which the drift parameter can be estimated can be derived from Equation 7 by finding the Δt that minimizes this expression (see Section 1.5 in the online supplementary material for the full derivation). In case the number of time point is large (say, $T > 100$), the following approximate result for the optimal SI holds[10]:

$$\Delta t_{opt} \approx \frac{-0.7968}{\alpha}. \tag{8}$$

The optimal SR with optimal SI Δt_{opt} for estimating the drift effect in a CT AR(1) model is thus a rather simple function of the population drift effect α, with larger effect sizes and hence lower autostabilities requiring faster SRs. The respective SIs can easily be calculated given the expected drift values. To generate such an expectation, one can rely on substantive theory, previous empirical findings or both. Figure 3 depicts the relationship between drift effect size and optimal SI over a broad range of plausible drift effects using the above approximate result (solid line; note that both axes are log-scaled).

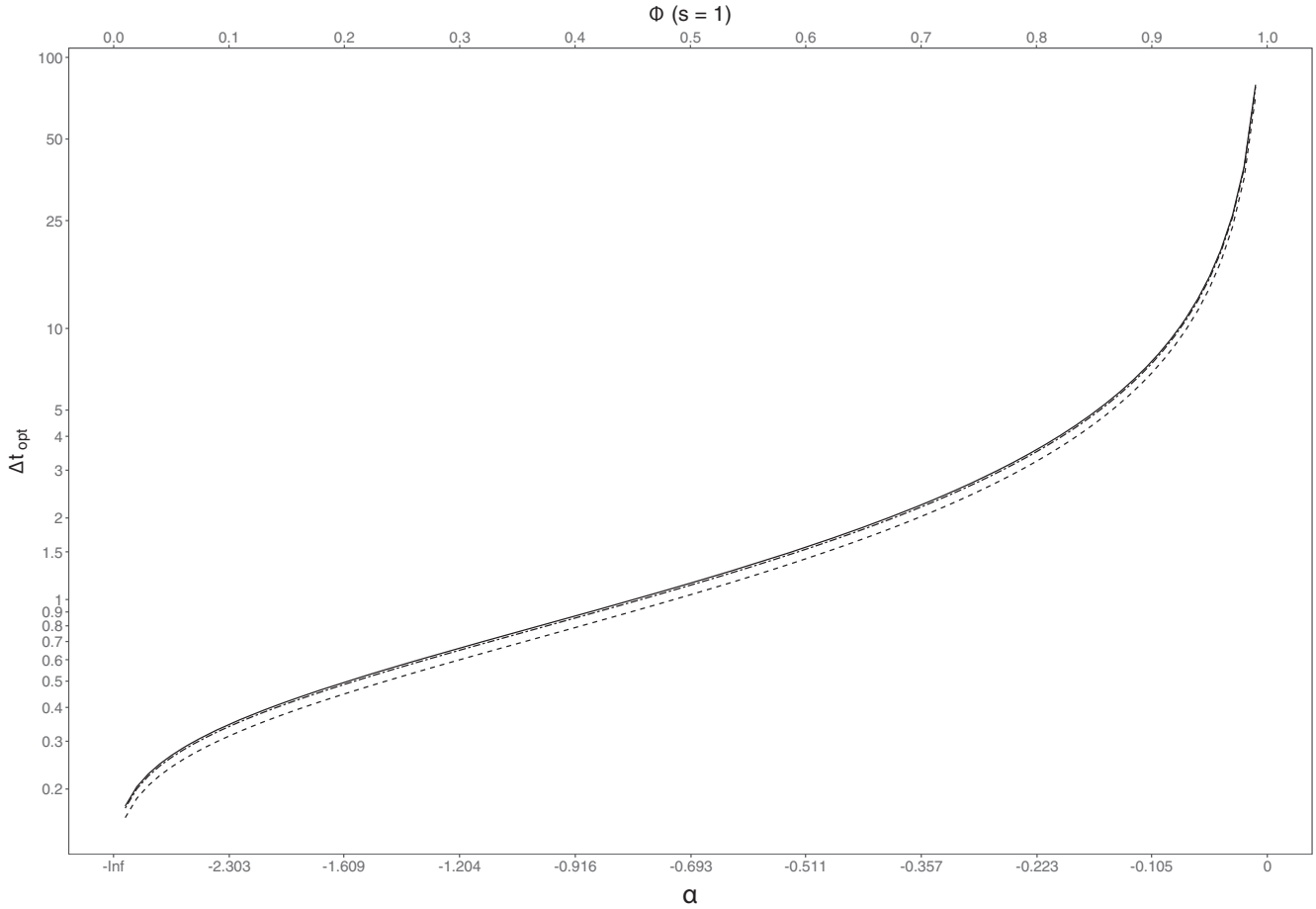
For smaller values of T, the numerator of Equation 8 is of slightly different value and dependent on T, resulting in slightly different optimal SIs (see the dashed and dash-dotted line in Figure 3, for two examples for $T = 10$ and $T = 50$). But it quickly converges toward the above value (see Figure 1 in the online supplementary material for a depiction). Table 1 in Section 1.5.2 in the online supplementary material presents numerator values for $T \in \{10, \ldots, 500\}$, which can be inserted in Equation 8 to determine accurate optimal SIs for shorter time series. Note the interesting implication that the optimal SI is practically independent of the total number of time points. That is, from a certain time series length on, the reliability of the drift estimator will always be minimal at the same SI for a given drift effect value, no matter how long the time series is.

Illustration With COGITO Data

Imagine we were planning an intensive longitudinal study to estimate the dynamics of NA and PA in a sample of younger individuals, during which we wanted to make use of the just-presented optimal SR-result. We thus first need some idea about which individual-specific drift effect values we can expect for our study. To come up with plausible effect sizes, we decide to rely on existing empirical work regarding affect dynamics and use the parameter estimates obtained from the COGITO data. All key results from this and the following subsections are displayed in Figure 4. A

[10] See Kenney et al. (2020) for an independent derivation of this result, published during the revision process of the present article.

Figure 3
Optimal SIs Over a Broad Range of Plausible Drift Effect Values



Note. The solid line depicts the approximate relationship for longer time series, the dash-dotted line, very close to the solid line, pertains to time series with 50 time points, the dashed line to time series with 10 time points. CT AR effect sizes on the lower x-axis and optimal SIs on the y-axis are displayed on a log scale. Implied DT AR effects for a time interval of one can be read from the upper x-axis.

table overviewing all modeling solutions included in the present article can be found in the online supplementary material (Table 3, Section 4.2).

In this section, we examine what the optimal SI would be and how much estimation reliability we could hypothetically gain if we consider the obtained CT AR(1) drift effect estimates individually. To do so, we first determine each participant's optimal SR based on the obtained drift estimate and Equation 8. We compare the optimal SI with the actual (i.e., median) SI to see how much faster (or slower) we would need to sample. We then calculate the "optimal" *SE*, so the *SE* that would be associated with the optimal SI via Equation 7. Finally, we compare this *SE* with the *SE* associated with the actual (i.e., median) SI to see how much better we could do in terms of drift estimator precision.

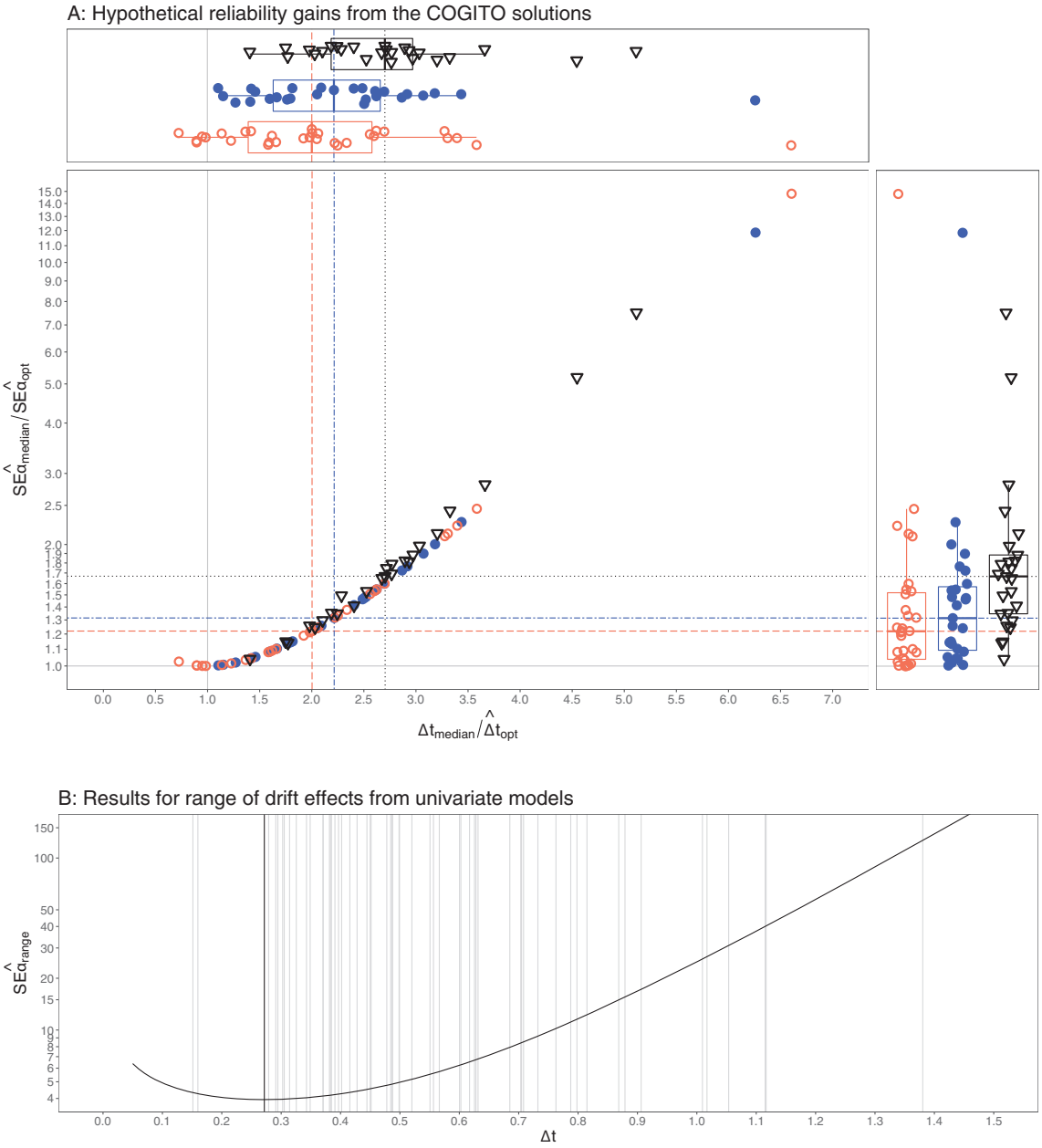
Taking the NA results presented in Figure 1 as an example, we obtained a drift estimate of $\hat{\alpha}_{1obs} = -0.58$, which yields an approximate optimal SI of $\hat{\Delta}t_{opt} \approx -0.7968/-.58 \approx 1.37$. We use the hat notation here because the SI is based on a parameter estimate, and thus an estimate as well. Because the drift estimate was obtained on basis of daily data (i.e., time entered the model scaled in days), the optimal SI also pertains to days. So, 1.37 days would be the optimal SI for this participant. The median SI Δt_{med} is one day, which means we would need to sample 1.37 times as slow ($\hat{\Delta}t_{opt}/\Delta t_{med} = 1.37/1$) or 0.73 times as fast ($\Delta t_{med}/\hat{\Delta}t_{opt} = 1/1.37 \approx 0.73$) as it was done in the median.[11] To determine the *SE*s associated with the optimal and median SIs, we again use our derived expression for the drift estimator variance. We insert the drift estimate, the number of actual time points (in this case $T = 101$), and either $\hat{\Delta}t_{opt}$ or Δt_{med} to obtain $SE_{\hat{\alpha}_{opt}} \approx 0.14$ and $SE_{\hat{\alpha}_{med}} \approx 0.15$. By sampling 1.37 times slower,

[11] Note that we use median SIs, simply because the SR of the COGITO data varies for each participant, while we need a single SI. And while the mean SI can be inflated by a single long study interruption, the median SI is more robust, and equals 1 day for all but two participants, for whom it equals 2 days. To match the median SI, we also use (theoretical) *SE*s that we calculate for the median SIs instead of the estimated *SE*s. However, doing this yields *SE*s that correlate highly with the ones obtained during model estimation for the cases included in the figure (i.e., $r > .99$).

This document is copyrighted by the American Psychological Association or one of its allied publishers.
This article is intended solely for the personal use of the individual user and is not to be disseminated broadly.

Figure 4

Application of the Optimal SR-Results to the Obtained COGITO Solutions



Note. Panel A shows hypothetical reliability gains as a function of SR-optimization based on the obtained COGITO modeling solutions. SR-optimization is displayed in terms of SR ratios, specifically ratios of actual median to optimal SIs, with the latter being calculated for the obtained drift effect estimates. Reliability gains are displayed on a log scale in terms of ratios of median to optimal drift effect *SE*s, calculated on basis of median and optimal SIs. Empty red circles mark NA results, filled blue circles PA results, and empty black triangles results pertaining to the CT VAR(1) modeling solutions. Vertical and horizontal lines mark ratios of one (gray solid lines), median NA ratios (dashed red lines), median PA ratios (dash-dotted blue lines), and median ratios pertaining to the multivariate modeling solutions (dotted black lines). Panel B shows the estimation reliability of a set of drift effects as a function of the SI. The set of drift effects thereby consists of all NA and PA drift estimates, and its estimation reliability is assessed in terms of the total drift *SE*, which equals the square root of the sum of all drift estimator variances in the set (again, displayed on a log scale). The optimal SI for the set is marked with a black vertical line. Gray vertical lines mark optimal SIs of all individual drift effects in the set. See the online article for the color version of this figure.

This document is copyrighted by the American Psychological Association or one of its allied publishers.
This article is intended solely for the personal use of the individual user and is not to be disseminated broadly.

we could thus improve estimation precision of the drift effect estimator by a factor of $SE_{\hat{\alpha}_{med}}/SE_{\hat{\alpha}_{opt}} \approx 1.07$.

Panel A of Figure 4 visualizes these comparisons for most obtained univariate COGITO solutions.[12] Ratios of the median to optimal SIs (i.e., SI changes) are thereby plotted along the *x*-axis, and ratios of median to optimal drift effect *SE*s (i.e., reliability gains) are plotted along the *y*-axis on a log scale. For now we only consider the circles in the plot, as the triangles pertain to the multivariate COGITO solutions and will be discussed later. Empty red circles pertain to NA modeling solutions and filled blue circles to PA solutions. Along both axes, the solid gray lines mark ratios of one, the dashed red lines mark the median of the NA ratios, and the dash-dotted blue lines mark the median PA ratio.

Looking at the distribution of all circles we see that, for some cases, both ratios are relatively close to one, revealing that the corresponding participants' affective experiences were sampled quite optimally already. For a number of participants, however, both ratios deviate substantially from one, indicating that estimation reliability could be improved upon—on average by factors of 1.22 (median NA ratio) and 1.32 (median PA ratio). This would require speeding up the median SR by average factors of 2.00 (median NA ratio) and 2.22 (median PA ratio). This would mean sampling multiple times a day, for some participants every couple of hours. Only for NA of a few participants could SRs be slowed down to obtain maximally reliable drift effect estimates, for instance, in case of the exemplary participant discussed earlier. In general, the differences between PA and NA results seem rather limited.

Optimal Sampling Rates for a Set of Drift Effects in the Univariate Model

Minimizing the Total Variance of a Set of Drift Effect Estimators

In the previous section, we were concerned with SIs that would enable maximally reliable estimation of individual drift effects as part of the CT AR(1) model. We showed that such optimal SIs are first and foremost a function of the population-level drift effect. For $T > 100$, there is an (approximate) one-to-one mapping between optimal SR and drift effect size, and thus a specific optimal SI for each drift effect size, as determined by Equation 8.

However, when planning a (new) study with multiple participants, there is usually no detailed prior information about individual participants available, and individual-specific SRs are not feasible. Instead, one might want to implement one SR that is as optimal as possible for the entire sample of participants and their likely different drift effects. Another reason for considering multiple drift effects simultaneously could be that, even for an $N = 1$ study, one is not certain which drift effect size one should expect, and would like to plan given a range of possible drift effects to accommodate this uncertainty.

Consequently, our optimization criterion has shifted. Instead of finding the Δt that minimizes the drift estimator variance expressed in Equation 7, we now aim to find the Δt that minimizes multiple instances of the expression simultaneously, where these instances differ in terms of α, resulting in the following aggregated expression

$$\sigma^2_{\hat{\alpha}_{total}} = \sum_{n=1}^{N} z_n \sigma^2_{\hat{\alpha}_n} = \sum_{n=1}^{N} z_n \left(- \frac{T e^{-2\alpha_n \Delta t} \left(e^{2\alpha_n \Delta t} - 1\right)^2}{\Delta t^2 (T-1)\left((T-2)e^{2\alpha_n \Delta t} - T\right)} \right), \tag{9}$$

where $\{\alpha_n; n \in 1, \ldots, N\}$ is the set expected drift effects of size N, $\{\sigma^2_{\hat{\alpha}_n}; n \in 1, \ldots, N\}$ is the set of associated drift estimator variances, and $\{z_n; n \in 1, \ldots, N\}$ is a set of weights which can be set to one if no differential weighting is desired.

To address this optimization problem, we use a numerical approach: Drawing upon basic optimization routines available in *R*, specifically the base-function *stats::optim(),* and its capability of gradient-based optimization, we have set up our own *R* function, which minimizes Equation 9 with respect to Δt. A demonstration of how to use the function, including an accuracy check, is presented in Section 2.1 of the online supplementary material (the annotated function code is available via the Open Science Framework project https://osf.io/zgebd/). Note that the tackled numerical optimization problem is simple (i.e., convex as can be seen from the to be discussed Panel B of Figure 4), can be solved fast (i.e., usually in a few seconds at maximum) and allows to handle all kinds of drift effect sets (e.g., quasi-continuous ranges vs. a few selected values).

Illustration With COGITO Data

To illustrate this optimal SR-result with the COGITO data we return to our hypothetical study planning scenario and examine what the optimal SR would be based on all univariate solutions. We thus subsume the obtained drift effect estimates as a set of population-level drift effects that we can plausibly expect, and hand it over to our *R* function. The result is depicted in Panel B of Figure 4 The black vertical line marks the optimal SI, which equals about .27 days. The gray vertical lines are added to locate the optimal SIs we would get for all drift values in the set individually. The curve shows the total *SE* for the set of drift estimators as a function of the SI. This total *SE* is an equivalent of the here-considered optimization criterion, the total variance of the set of drift estimators. It is obtained by taking the square root of Equation 9.

Remarkably, the optimal SI for the drift range is rather small. It approaches the optimal SI associated with the largest drift effect implying the lowest autostability, and is substantially smaller than the average of the individual optimal SIs (i.e., the mean of the individual optimal SIs is .57, the median is .50). To understand why this is the case, it is useful to revisit Panel A of Figure 2, and remind oneself of how quickly slowing down the SR could deteriorate the drift estimator's reliability in case of large population-level drift values, and how much less reliabilities were affected given smaller drift values. Now large and small drift values are taken together as a set, and so are the associated reliability losses caused by any SI that is not optimal. Because there practically is a one-to-one relationship between drift size and optimal SI, all

[12] A few solutions are not included in the figure and are indicated as such in Table 3 in the online supplementary material. These were cases with extremely large drift effect values, for whom we thus obtain *SE* and SI ratios so extreme that the figure would not have been readable anymore. For some of the affected multivariate solutions, we could not obtain optimal SRs, because the FI matrix was computationally singular and could therefore not be inverted during optimization.

This document is copyrighted by the American Psychological Association or one of its allied publishers.
This article is intended solely for the personal use of the individual user and is not to be disseminated broadly.

possible SIs will be suboptimal for either all or all but one drift value in the set. However, we can still try to find the SI that balances the set of reliability losses such that it is least suboptimal for the set of drift values. This figural take on the problem should clarify why higher losses will have relatively more impact than lower losses, and thus why larger drift effects and the associated shorter optimal SIs are reflected more in drift-range optimal SR.

Optimal Sampling Rates for Reliable Drift Matrix Estimation in the Multivariate Model

Minimizing the Total Variance of the Drift Matrix Estimators

Turning to the CT VAR(1) model, we now aim to estimate the whole matrix of drift effects with maximal precision. For the bivariate model variant, the optimization target thus becomes

$$\sigma^2_{\hat{A}} = \sigma^2_{\hat{\alpha}_{11}} + \sigma^2_{\hat{\alpha}_{21}} + \sigma^2_{\hat{\alpha}_{12}} + \sigma^2_{\hat{\alpha}_{22}}, \quad (10)$$

which is also the trace of that block of the model's FI-based parameter covariance matrix that pertains to the drift effects. Note that the trace of the parameter covariance matrix is a common optimization target in OD theory applications in situations where multiple parameters are of interest (Pronzato, 2008).

Unlike for the univariate case, it was not feasible to derive analytical expressions for the parameter variances and covariances for the multivariate model. Thus, we again take a numerical approach: Relying on the same numerical optimization machinery as before (i.e., *stats::optim()*) and the exact FI matrix expression derived in Equation 18 in the online supplementary material, we set up an *R* function that allows to find the optimal SI for reliable estimation of all AR and CR drift effects in a bivariate CT VAR(1) model. As with the previous *R* function, a demonstration and an accuracy check are included in the online supplementary material (Section 2.2), and the code is again available via the Open Science Framework project.

Illustration With COGITO Data

In this section, we again consider the obtained modeling solutions individually, and the hypothetical reliability gains are displayed in Panel A of Figure 4 That is, per individual participant, we are again investigate how much faster than their median SR we would have to sample in order to minimize the total estimation variance across all drift effect estimators and its square root as a measure of the total *SE*, respectively. In the figure, the factors by which the SRs would have to be accelerated are plotted along the *x*-axis, and the factors by which the total *SE*s would improve as compared with the total *SE*s based on the median SIs are plotted along the *y*-axis. We now focus on the triangles representing the results for the multivariate modeling solutions.

Compared with the univariate results, we observe a shift for the majority of both SI and SR ratios. The median SI ratio now equals 2.70, while the median *SE* ratio equals 1.67. Thus, if we sampled on average 2.70 times faster, we would obtain drift estimators that were on average 1.67 times more reliable. Because the data and their actual sampling scheme remain the same, we can conclude that SRs required for maximally reliable CT VAR(1) results are faster than those for maximally reliable CT AR(1) results. In part, this result is driven by the principle that underlay the results in the previous section: Also in the VAR case we are integrating across a set of drift effects in some way. In this set, those effects that imply lower autostabilities—and probably also those effects implying lower cross-stabilities—will be the ones determining (shorter) optimal SIs, as their estimation is most affected by suboptimal SIs. The exact interaction of the different drift effect sizes in the transition matrix in determining the optimal SI is of course more complicated than in the case of a range of drift effects in the univariate context. Also the process error variances and covariances seem to play a role. Some exemplary parameter settings are studied in Section 1.6 in the online supplementary material.

Discussion

Summary

In the present article, we investigate the effect of the SR of intensive longitudinal data on the estimation reliability of the CT AR(1) and VAR(1) model. To assess estimation reliability, we rely on ML estimation theory and the inverted FI matrix. We derive analytical expressions for the (inverted) FI matrix for the univariate and multivariate model, and show how the SR affects reliability of the models' parameter estimators. For the CT AR(1) model, the magnitude and shape of these effects depend strongly on the population-level drift effect and hence the autostability of the to-be-estimated process. Undersampling may thus have severe consequences, especially in case of lower autostabilities (larger drift-effects), in that it may lead to low precision and distinguishability. For the bivariate CR VAR(1) model, analogous patterns arise, although the complexity of the problem is increased due to the multivariate model structure. In a next step, we show how to determine optimal SIs for maximally reliable estimation of the drift effects in the discussed models. We thereby focus on three scenarios: estimation of a single drift effect as well as a set of drift effects in the context of the univariate model, and estimation of the matrix of drift effects in the context of the bivariate model. Basically, optimal SIs can be obtained on basis of expected population parameter values, either via an explicit and simple analytical expression for the estimation of a single drift value, or via standard numerical optimization routines. We provide the relevant expressions and *R* functions, and illustrate our results based on data from the COGITO Study.

Strengths and Limitations of the Employed Approach

First, in the present article, we determine reliability-optimal SRs for the CT AR(1) and VAR(1) model based on theory, OD theory to motivate estimation reliability as an optimality criterion, and, more importantly, ML estimation theory to motivate the use of the inverted FI as a reliability measure. On the one hand, this can be considered a limitation: ML estimation theory is asymptotic, that is, formulated in the context of indefinitely growing sample sizes. The results we obtain here thus pertain to the behavior of parameter estimators if sample sizes get large, because only then the inverted FI provides for an exact measure of estimator (co)variances. While the asymptotic approach is an established one in studying the performance of estimators (Lehmann & Casella, 1998), it also means that, in finite samples (i.e., shorter time series), our

This document is copyrighted by the American Psychological Association or one of its allied publishers.
This article is intended solely for the personal use of the individual user and is not to be disseminated broadly.

This document is copyrighted by the American Psychological Association or one of its allied publishers.
This article is intended solely for the personal use of the individual user and is not to be disseminated broadly.

results represent approximations. Their accuracy might then be impaired significantly if samples get too small (e.g., leading to finite sample biases) and if (in addition) ML estimation theory assumptions are violated (e.g., parameter values might not lie in the interior of the parameter space, possibly rendering their estimators' distributions non-normal; Pek & Wu, 2015). On the other hand, being based on theory also constitutes a strength of our approach: While our results pertain to rather ideal conditions, they also afford a general picture of the role of the SR for CT AR(1) and VAR(1) model estimation that we would otherwise not have been able to draw. Under less ideal conditions, it is of course possible to revert to alternative approaches to study the problem, usually simulation-based approaches, which are often used for power-optimal study planning (Maxwell et al., 2008). The opportunities of simulation-based approaches are mainly grounded in their larger flexibility. For instance, it is possible to explicitly study deviations from ML estimation theory, such as small sample sizes and miss-specified models. In addition and under the chosen simulation conditions, measures of estimation reliability can actually be evaluated, also alternatives to the FI-based one, such as resampling-based (e.g., bootstrapping; Efron, 1981) or likelihood-based ones (Neale & Miller, 1997; Pek & Wu, 2015). Such measures can be more robust toward various distortions, but are also computationally intensive and their accuracy is worse in smaller samples (Pek & Wu, 2015). However, it should be kept in mind that simulation-based approaches are always limited to a relatively small number of selected experimental conditions (e.g., selected parameter values) and affected by sampling error or even systematic drop out due to convergence failures. They will thus clearly benefit from having a general theoretical foundation of the sort we aimed to establish here. But they can be a valid next step in studying the optimal SR problem.

Second, we confine this paper to relatively simple AR and VAR model structures. More complex models involve extensions such as higher-order AR and CR effects, measurement models, nonstationary models with time varying parameters, or hierarchical model structures to accommodate multiple individuals simultaneously (e.g., Bringmann et al., 2013; Chow, 2019; Driver & Voelkle, 2018a; Hamaker & Dolan, 2009; Oud & Delsing, 2010). On the one hand, this restricts the scope of our results, as more complicated models pose their own, differential optimal SR problems, which we do thus not address in the present article. On the other hand, the principled problem remains somewhat invariant across different VAR-type models, and the basic understanding gained in the present article can be built upon in future accounts of more complex models. In addition, even if a more complex (i.e., higher-order or nonstationary) model is theoretically plausible, the more parsimonious model variants discussed here might in some cases still be interesting to control for overfitting of the data (cf. Bulteel et al., 2018).

Third, not only on the modeling side but also on the study design side, we limit complexity. For instance, we only looked at constant, time-invariant SIs with equidistant measurement occasions, neglecting the case of time-varying, random SRs (see Voelkle & Oud, 2013). Also, multiple study design factors could be targeted simultaneously. Already in our case, the total number of observations mattered for estimation reliability in addition to the SR—although we could show, that optimal SR decisions remain practically unaffected. If multiple study factors are considered simultaneously, their relative importance and trade-offs become of interest (cf. Brandmaier et al., 2015; von Oertzen, 2010; von Oertzen & Brandmaier, 2013). This also broadens the scope to taking into account not only the optimality of study design decisions, but also the suboptimality of study design restrictions (e.g., larger measurement intervals due to night breaks) and how they can be compensated for.

Fourth, we confined this article to a specific estimation method, formulation, and parameterization of the CT AR(1) and VAR(1) model. However, ML estimation is widely used due to its desirable properties and allows the implementation and estimation of VAR-type models in multivariate frameworks such as SEM and SSM, which feature flexible covariance and mean structure decompositions including common and specific latent variables, and can accommodate the more complicated model structures mentioned above. The formulation and parameterization chosen are the ones described in recent articles on CT VAR modeling (e.g., Driver et al., 2017; Voelkle et al., 2012); and bear resemblance to typical DT AR(1) and VAR(1) model formulations and parameterizations. Alternative estimation methods that also come with alternative formulations and parameterizations include fitting model variants with linear parameter constraints to highly oversampled data (Asparouhov et al., 2018; Singer, 2012) or estimating derivatives via filtering procedures and modeling these (Boker, 2012). These approaches avoid nonlinear parameter constraints (that can pose computational challenges; Voelkle et al., 2019) and rely on linear approximations. It is likely that alternative parameterizations, formulations, and estimation methods possess alternative estimation reliability characteristics (cf. von Oertzen & Boker, 2010).

Fifth, in our empirical illustration we used the obtained drift estimates to calculate optimal SIs, rendering them estimates too. The estimation variance of the drift effect estimator thus propagates to the optimal SI estimator, and, ironically, renders our optimal SR results for reliable drift effect estimation unreliable. This problem of propagation of (estimation) uncertainty has been discussed in the literature on statistical power calculations (e.g., Gelman & Carlin, 2014). In addition, uncertainty or variability in empirical results can also be caused by often somewhat arbitrary preprocessing decisions, implying a multiverse of data sets, and hence also a multiverse of eventual analysis results (Steegen et al., 2016). In this case, we for instance decided to use average scores excluding a number of NA items and to remove potential mean trends in a certain way (i.e., using local polynomial regression modeling with a certain smoothing span). One recommendation to circumvent the intricacies of estimating expected effect sizes from (limited) data is to rely on substantive theory instead. However, substantive theory can of course also be subject to uncertainties. As one pathway to directly accommodate uncertainty during study planning, be it due to analysis decisions, effect estimation, or lack of precision of substantive theories, we have introduced and studied the problem of optimal SIs across a set of possible drift effects.

Sixth and finally, we approached the problem of appropriate SRs from a statistical angle, tying it to the reliability with which a CT AR(1) and VAR(1) model, and especially their drift effects, can be estimated. On the one hand, this posits a clear criterion for determining the appropriateness of a SR. On the other hand, it constrains the appropriateness of a SR to the appropriateness of the CT AR(1) and VAR(1) model. In addition, it requires a-priori knowledge about the population-level auto- and cross-stabilities of

the psychological processes of interest. Alternative approaches to the problem of appropriate SRs and time scales might revolve around upstream issues of appropriate theory, measurement, or modeling, the consideration of which needs to complement—or even proceed—fitting a specific dynamic model to the data. Questions might be: What is the autostability of a given process, which units does the time scale possess at which the process unfolds and best reveals it's dynamics (e.g., minutes, hours, days)? How should measurements (e.g., item content) be designed to match a given process and time scale? At which time scales do measurement artefacts and errors evolve? Is a phenomenon indeed best described by a time-continuous process that is homogeneous in the sense that it develops along a single time scale, or are we instead dealing with multiple overlaying processes at multiple time scales, or one process at varying time scales, or time-discrete processes? What would be appropriate statistical modeling approaches? These are interesting aspects or redefinitions of the indeed complex problem of appropriate SRs, which we left unattended in the present article.

Conclusion

In the present article, we draw upon OD and ML estimation theory to show how the SR of intensive longitudinal data affects the estimation reliability of the CT AR(1) and VAR(1) model, and how optimal SIs can be determined. The relevant analytical expressions are provided here, *R* functions for numerical optimization are available. We believe that this article provides a useful basis for further research on optimal SRs for reliable VAR-type modeling of psychological processes. Optimizing future intensive longitudinal studies with respect to estimation reliability is important as it has immediate (e.g., model-based inference) but also more far-reaching consequences (e.g., generalizability of results) for research on psychological dynamics.

References

Adolf, J. K. (2018). *Contextualizing the dynamics of affective functioning: Conceptual and statistical considerations* [Doctoral dissertation]. Humboldt–Universität zu Berlin. https://doi.org/10.18452/19412

Asparouhov, T., Hamaker, E. L., & Muthén, B. (2018). Dynamic structural equation models. *Structural Equation Modeling*, *25*(3), 359–388. https://doi.org/10.1080/10705511.2017.1406803

Boker, S. M. (2002). Consequences of continuity: The hunt for intrinsic properties within parameters of dynamics in psychological processes. *Multivariate Behavioral Research*, *37*(3), 405–422. https://doi.org/10.1207/S15327906MBR3703_5

Boker, S. M. (2012). Dynamical systems and differential equation models of change. In H. Cooper, P. M. Camic, D. L. Long, A. T. Panter, D. Rindskopf, & K. J. Sher (Eds.), *APA handbook of research methods in psychology, Vol 3: Data analysis and research publication* (pp. 323–333). American Psychological Association. https://doi.org/10.1037/13621-016

Bolger, N., Davis, A., & Rafaeli, E. (2003). Diary methods: Capturing life as it is lived. *Annual Review of Psychology*, *54*(1), 579–616. https://doi.org/10.1146/annurev.psych.54.101601.145030

Brandmaier, A. M., von Oertzen, T., Ghisletta, P., Hertzog, C., & Lindenberger, U. (2015). LIFESPAN: A tool for the computer-aided design of longitudinal studies. *Frontiers in Psychology*, *6*, 272. https://doi.org/10.3389/fpsyg.2015.00272

Brandmaier, A. M., von Oertzen, T., Ghisletta, P., Lindenberger, U., & Hertzog, C. (2018). Precision, reliability, and effect size of slope variance in latent growth curve models: Implications for statistical power analysis. *Frontiers in Psychology*, *9*, 294. https://doi.org/10.3389/fpsyg.2018.00294

Bringmann, L. F., Pe, M. L., Vissers, N., Ceulemans, E., Borsboom, D., Vanpaemel, W., Tuerlinckx, F., & Kuppens, P. (2016). Assessing temporal emotion dynamics using networks. *Assessment*, *23*(4), 425–435. https://doi.org/10.1177/1073191116645909

Bringmann, L. F., Vissers, N., Wichers, M., Geschwind, N., Kuppens, P., Peeters, F., Borsboom, D., & Tuerlinckx, F. (2013). A network approach to psychopathology: New insights into clinical longitudinal data. *PLoS ONE*, *8*(4), e60188. https://doi.org/10.1371/journal.pone.0060188

Brose, A., Schmiedek, F., Koval, P., & Kuppens, P. (2015). Emotional inertia contributes to depressive symptoms beyond perseverative thinking. *Cognition and Emotion*, *29*(3), 527–538. https://doi.org/10.1080/02699931.2014.916252

Brose, A., Schmiedek, F., Lövdén, M., & Lindenberger, U. (2012). Daily variability in working memory is coupled with negative affect: The role of attention and motivation. *Emotion*, *12*(3), 605–617. https://doi.org/10.1037/a0024436

Bulteel, K., Mestdagh, M., Tuerlinckx, F., & Ceulemans, E. (2018). VAR (1) based models do not always outpredict AR(1) models in typical psychological applications. *Psychological Methods*, *23*(4), 740–756. https://doi.org/10.1037/met0000178

Chow, S.-M. (2019). Practical tools and guidelines for exploring and fitting linear and nonlinear dynamical systems models. *Multivariate Behavioral Research*, *54*(5), 690–718. https://doi.org/10.1080/00273171.2019.1566050

Chow, S.-M., Ram, N., Boker, S. M., Fujita, F., & Clore, G. (2005). Emotion as a thermostat: Representing emotion regulation using a damped oscillator model. *Emotion*, *5*(2), 208–225. https://doi.org/10.1037/1528-3542.5.2.208

Cleveland, W. S., Grosse, E., & Shyu, W. M. (1993). Local regression models. In J. M. Chambers & T. J. Hastie (Eds.), *Statistical models in S* (pp. 309–376). Chapman & Hall.

De Haan-Rietdijk, S., Gottman, J. M., Bergeman, C. S., & Hamaker, E. L. (2016). Get over it! A multilevel threshold autoregressive model for state-dependent affect regulation. *Psychometrika*, *81*(1), 217–241. https://doi.org/10.1007/s11336-014-9417-x

Deboeck, P. R., & Preacher, K. J. (2016). No need to be discrete: A method for continuous time mediation analysis. *Structural Equation Modeling*, *23*(1), 61–75. https://doi.org/10.1080/10705511.2014.973960

Dobos, L., & Abonyi, J. (2013). Fisher information matrix based time-series segmentation of process data. *Chemical Engineering Science*, *101*, 99–108. https://doi.org/10.1016/j.ces.2013.06.030

Driver, C. C., Oud, J. H. L., & Voelkle, M. C. (2017). Continuous time structural equation modelling with R Package ctsem. *Journal of Statistical Software*, *77*(5), 1–35. https://doi.org/10.18637/jss.v077.i05

Driver, C. C., & Voelkle, M. C. (2018a). Hierarchical Bayesian continuous time dynamic modeling. *Psychological Methods*, *23*(4), 774–799. https://doi.org/10.1037/met0000168

Driver, C. C., & Voelkle, M. C. (2018b). Understanding the time course of interventions with continuous time dynamic models. In K. van Montfort, J. H. L. Oud, & M. C. Voelkle (Eds.), *Continuous time modeling in the behavioral and related sciences* (pp. 79–109). Springer International Publishing. https://doi.org/10.1007/978-3-319-77219-6_4

Efron, B. (1981). Nonparametric estimates of standard error—The jackknife, the bootstrap and other methods. *Biometrika*, *68*(3), 589–599. https://doi.org/10.1093/biomet/68.3.589

Eisenberg, M. C., & Hayashi, M. A. L. (2014). Determining identifiable parameter combinations using subset profiling. *Mathematical Biosciences*, *256*, 116–126. https://doi.org/10.1016/j.mbs.2014.08.008

Enders, C. K. (2010). *Applied missing data analysis*. Guilford Press.

This document is copyrighted by the American Psychological Association or one of its allied publishers.
This article is intended solely for the personal use of the individual user and is not to be disseminated broadly.

This document is copyrighted by the American Psychological Association or one of its allied publishers.
This article is intended solely for the personal use of the individual user and is not to be disseminated broadly.

Gelman, A., & Carlin, J. (2014). Beyond power calculations: Assessing Type S (sign) and Type M (magnitude) errors. *Perspectives on Psychological Science*, *9*(6), 641–651. https://doi.org/10.1177/1745691614 551642

Hamaker, E. L., & Dolan, C. V. (2009). Idiographic data analysis: Quantitative methods—From simple to advanced. In J. Valsiner, P. C. M. Molenaar, M. C. D. P. Lyra, & N. Chaudhary (Eds.), *Dynamic process methodology in the social and behavioral sciences* (pp. 191–216). Springer. https://doi.org/10.1007/978-0-387-95922-1_9

Hamaker, E. L., & Wichers, M. (2017). No time like the present: Discovering the hidden dynamics in intensive longitudinal data. *Current Directions in Psychological Science*, *26*(1), 10–15. https://doi.org/10.1177/0963721416666518

Hamaker, E. L., Ceulemans, E., Grasman, R. P. P. P., & Tuerlinckx, F. (2015). Modeling affect dynamics: State of the art and future challenges. *Emotion Review*, *7*(4), 316–322. https://doi.org/10.1177/1754073915 590619

Hamilton, J. D. (1994). *Time series analysis* (2nd ed.). Princeton University Press. https://doi.org/10.1515/9780691218632

Harvey, A. C. (1989). *Forecasting, Structural time series models and the Kalman Filter*. Cambridge University Press.

Hunter, M. D. (2018). State space modeling in an open source, modular, structural equation modeling environment. *Structural Equation Modeling*, *25*(2), 307–324. https://doi.org/10.1080/10705511.2017.1369354

Karch, J. (2016). *A machine learning perspective on repeated measures*. Humboldt-Universität zu Berlin, Lebenswissenschaftliche Fakultät. https://doi.org/10.18452/17641

Kenney, T., Gao, J., & Gu, H. (2020). Application of OU processes to modelling temporal dynamics of the human microbiome, and calculating optimal sampling schemes. *BMC Bioinformatics*, *21*, 450. https://doi.org/10.1186/s12859-020-03747-4

Koval, P., Brose, A., Pe, M. L., Houben, M., Erbas, Y., Champagne, D., & Kuppens, P. (2015). Emotional inertia and external events: The roles of exposure, reactivity, and recovery. *Emotion*, *15*(5), 625–636. https://doi.org/10.1037/emo0000059

Kuiper, R. M., & Ryan, O. (2018). Drawing conclusions from cross-lagged relationships: Re-considering the role of the time-interval. *Structural Equation Modeling*, *25*(5), 809–823. https://doi.org/10.1080/10705511.2018.1431046

Kuppens, P., Allen, N. B., & Sheeber, L. B. (2010). Emotional inertia and psychological maladjustment. *Psychological Science*, *21*(7), 984–991. https://doi.org/10.1177/0956797610372634

Kuppens, P., & Verduyn, P. (2015). Looking at emotion regulation through the window of emotion dynamics. *Psychological Inquiry*, *26*(1), 72–79. https://doi.org/10.1080/1047840X.2015.960505

Lehmann, E. L., & Casella, G. (1998). *Theory of point estimation* (2nd ed.). Springer.

Liu, X. S. (2012). Implications of statistical power for confidence intervals: Statistical power and confidence intervals. *British Journal of Mathematical & Statistical Psychology*, *65*(3), 427–437. https://doi.org/10.1111/j.2044-8317.2011.02035.x

Lütkepohl, H. (2005). *New introduction to multiple time series analysis*. Springer. https://doi.org/10.1007/978-3-540-27752-1

Ly, A., Marsman, M., Verhagen, J., Grasman, R. P. P. P., & Wagenmakers, E.-J. (2017). A tutorial on Fisher information. *Journal of Mathematical Psychology*, *80*, 40–55. https://doi.org/10.1016/j.jmp.2017.05.006

Maxwell, S. E., Kelley, K., & Rausch, J. R. (2008). Sample size planning for statistical power and accuracy in parameter estimation. *Annual Review of Psychology*, *59*(1), 537–563. https://doi.org/10.1146/annurev.psych.59.103006.093735

Myung, I. J. (2003). Tutorial on maximum likelihood estimation. *Journal of Mathematical Psychology*, *47*(1), 90–100. https://doi.org/10.1016/S0022-2496(02)00028-7

Neale, M. C., Hunter, M. D., Pritikin, J. N., Zahery, M., Brick, T. R., Kirkpatrick, R. M., Estabrook, R., Bates, T. C., Maes, H. H., & Boker, S. M. (2016). OpenMx 2.0: Extended structural equation and statistical modeling. *Psychometrika*, *81*(2), 535–549. https://doi.org/10.1007/s11336-014-9435-8

Neale, M. C., & Miller, M. B. (1997). The use of likelihood-based confidence intervals in genetic models. *Behavior Genetics*, *27*(2), 113–120. https://doi.org/10.1023/A:1025681223921

Oravecz, Z., Tuerlinckx, F., & Vandekerckhove, J. (2011). A hierarchical latent stochastic differential equation model for affective dynamics. *Psychological Methods*, *16*(4), 468–490. https://doi.org/10.1037/a0024375

Oud, J. H. L., & Delsing, M. J. M. H. (2010). Continuous time modeling of panel data by means of SEM. In K. v. Montfort, J. H. L. Oud, & A. Satorra (Eds.), *Longitudinal research with latent variables* (pp. 201–244). Springer. https://doi.org/10.1007/978-3-642-11760-2_7

Pe, M. L., & Kuppens, P. (2012). The dynamic interplay between emotions in daily life: Augmentation, blunting, and the role of appraisal overlap. *Emotion*, *12*(6), 1320–1328. https://doi.org/10.1037/a0028262

Pek, J., & Wu, H. (2015). Profile likelihood-based confidence intervals and regions for structural equation models. *Psychometrika*, *80*(4), 1123–1145. https://doi.org/10.1007/s11336-015-9461-1

Pronzato, L. (2008). Optimal experimental design and some related control problems. *Automatica*, *44*(2), 303–325. https://doi.org/10.1016/j.automatica.2007.05.016

R Core Team. (2017). R: A language and environment for statistical computing (Version 3.6.1) [Computer software]. R Foundation for Statistical Computing. https://www.R-project.org/

Ryan, O., Kuiper, R. M., & Hamaker, E. L. (2018). A continuous-time approach to intensive longitudinal data: What, why, and how? In K. van Montfort, J. H. L. Oud, & M. C. Voelkle (Eds.), *Continuous time modeling in the behavioral and related sciences* (pp. 27–54). Springer International Publishing. https://doi.org/10.1007/978-3-319-77219-6_2

Schmiedek, F., Lövdén, M., & Lindenberger, U. (2010). Hundred days of cognitive training enhance broad cognitive abilities in adulthood: Findings from the COGITO study. *Frontiers in Aging Neuroscience*, *2*, 27. https://doi.org/10.3389/fnagi.2010.00027

Schuurman, N. K., Houtveen, J. H., & Hamaker, E. L. (2015). Incorporating measurement error in n = 1 psychological autoregressive modeling. *Frontiers in Psychology*, *6*, 1038. https://doi.org/10.3389/fpsyg.2015.01038

Shardt, Y. A. W., & Huang, B. (2013). Data quality assessment of routine operating data for process identification. *Computers & Chemical Engineering*, *55*, 19–27. https://doi.org/10.1016/j.compchemeng.2013.03.029

Singer, H. (2012). SEM modeling with singular moment matrices Part II: ML-estimation of sampled stochastic differential equations. *The Journal of Mathematical Sociology*, *36*(1), 22–43. https://doi.org/10.1080/0022250X.2010.532259

Steegen, S., Tuerlinckx, F., Gelman, A., & Vanpaemel, W. (2016). Increasing transparency through a multiverse analysis. *Perspectives on Psychological Science*, *11*(5), 702–712. https://doi.org/10.1177/174569161 6658637

Suls, J., Green, P., & Hillis, S. (1998). Emotional reactivity to everyday problems, affective inertia, and neuroticism. *Personality and Social Psychology Bulletin*, *24*(2), 127–136. https://doi.org/10.1177/0146167298242002

Trull, T. J., Lane, S. P., Koval, P., & Ebner-Priemer, U. W. (2015). Affective dynamics in psychopathology. *Emotion Review*, *7*(4), 355–361. https://doi.org/10.1177/1754073915590617

Vanlier, J., Tiemann, C. A., Hilbers, P. A. J., & van Riel, N. A. W. (2012). An integrated strategy for prediction uncertainty analysis. *Bioinformatics*, *28*(8), 1130–1135. https://doi.org/10.1093/bioinformatics/bts088

Voelkle, M. C., & Oud, J. H. L. (2013). Continuous time modelling with individually varying time intervals for oscillating and non-oscillating processes: Continuous time modelling. *British Journal of Mathematical & Statistical Psychology*, *66*(1), 103–126. https://doi.org/10.1111/j.2044-8317.2012.02043.x

Voelkle, M. C., Brose, A., Schmiedek, F., & Lindenberger, U. (2014). Toward a unified framework for the study of between-person and within-

person structures: Building a bridge between two research paradigms. *Multivariate Behavioral Research*, *49*(3), 193–213. https://doi.org/10.1080/00273171.2014.889593

Voelkle, M. C., Oud, J. H. L., Davidov, E., & Schmidt, P. (2012). An SEM approach to continuous time modeling of panel data: Relating authoritarianism and anomia. *Psychological Methods*, *17*(2), 176–192. https://doi.org/10.1037/a0027543

Voelkle, M. C., Gische, C., Driver, C. C., & Lindenberger, U. (2019). The role of time in the quest for understanding psychological mechanisms. *Multivariate Behavioral Research*, *53*(6), 782–805. https://doi.org/10.1080/00273171.2018.1496813

von Oertzen, T. (2010). Power equivalence in structural equation modelling. *British Journal of Mathematical & Statistical Psychology*, *63*(2), 257–272. https://doi.org/10.1348/000711009X441021

von Oertzen, T., & Boker, S. M. (2010). Time delay embedding increases estimation precision of models of intraindividual variability. *Psychometrika*, *75*(1), 158–175. https://doi.org/10.1007/s11336-009-9137-9

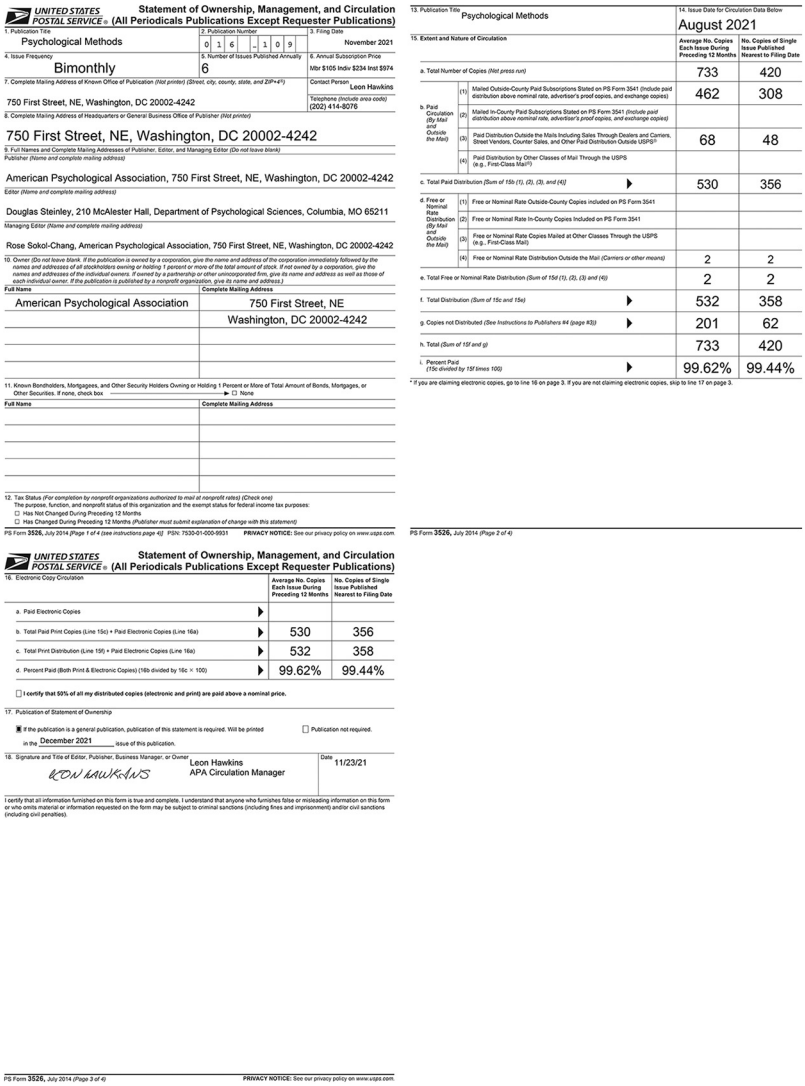
von Oertzen, T., & Brandmaier, A. M. (2013). Optimal study design with identical power: An application of power equivalence to latent growth curve models. *Psychology and Aging*, *28*(2), 414–428. https://doi.org/10.1037/a0031844

Watson, D., Clark, L. A., & Tellegen, A. (1988). Development and validation of brief measures of positive and negative affect: The PANAS scales. *Journal of Personality and Social Psychology*, *54*(6), 1063–1070. https://doi.org/10.1037/0022-3514.54.6.1063

Wolfram Research, Inc. (2018). Mathematica (Version 11.3) [Computer software]. https://www.wolfram.com/mathematica

Received August 8, 2019
Revision received January 8, 2021
Accepted January 11, 2021 ■

This document is copyrighted by the American Psychological Association or one of its allied publishers.
This article is intended solely for the personal use of the individual user and is not to be disseminated broadly.



UNITED STATES POSTAL SERVICE® Statement of Ownership, Management, and Circulation (All Periodicals Publications Except Requester Publications)

1. Publication Title: Psychological Methods
2. Publication Number: 0 1 6 – 1 0 9
3. Filing Date: November 2021
4. Issue Frequency: Bimonthly
5. Number of Issues Published Annually: 6
6. Annual Subscription Price: Mbr $105 Indiv $234 Inst $974
7. Complete Mailing Address of Known Office of Publication (Not printer) (Street, city, county, state, and ZIP+4®): 750 First Street, NE, Washington, DC 20002-4242
Contact Person: Leon Hawkins
Telephone (Include area code): (202) 414-8076
8. Complete Mailing Address of Headquarters or General Business Office of Publisher (Not printer): 750 First Street, NE, Washington, DC 20002-4242
9. Full Names and Complete Mailing Addresses of Publisher, Editor, and Managing Editor (Do not leave blank)
Publisher (Name and complete mailing address): American Psychological Association, 750 First Street, NE, Washington, DC 20002-4242
Editor (Name and complete mailing address): Douglas Steinley, 210 McAlester Hall, Department of Psychological Sciences, Columbia, MO 65211
Managing Editor (Name and complete mailing address): Rose Sokol-Chang, American Psychological Association, 750 First Street, NE, Washington, DC 20002-4242
10. Owner (Do not leave blank. If the publication is owned by a corporation, give the name and address of the corporation immediately followed by the names and addresses of all stockholders owning or holding 1 percent or more of the total amount of stock. If not owned by a corporation, give the names and addresses of the individual owners. If owned by a partnership or other unincorporated firm, give its name and address as well as those of each individual owner. If the publication is published by a nonprofit organization, give its name and address.)

Full Name	Complete Mailing Address
American Psychological Association	750 First Street, NE Washington, DC 20002-4242

11. Known Bondholders, Mortgagees, and Other Security Holders Owning or Holding 1 Percent or More of Total Amount of Bonds, Mortgages, or Other Securities. If none, check box → ☐ None

Full Name	Complete Mailing Address

12. Tax Status (For completion by nonprofit organizations authorized to mail at nonprofit rates) (Check one)
The purpose, function, and nonprofit status of this organization and the exempt status for federal income tax purposes:
☐ Has Not Changed During Preceding 12 Months
☐ Has Changed During Preceding 12 Months (Publisher must submit explanation of change with this statement)

PS Form 3526, July 2014 (Page 1 of 4 (see instructions page 4)) PSN: 7530-01-000-9931 PRIVACY NOTICE: See our privacy policy on www.usps.com.

13. Publication Title: Psychological Methods
14. Issue Date for Circulation Data Below: August 2021

15. Extent and Nature of Circulation			Average No. Copies Each Issue During Preceding 12 Months	No. Copies of Single Issue Published Nearest to Filing Date
a. Total Number of Copies (Net press run)			733	420
b. Paid Circulation (By Mail and Outside the Mail)	(1)	Mailed Outside-County Paid Subscriptions Stated on PS Form 3541 (Include paid distribution above nominal rate, advertiser's proof copies, and exchange copies)	462	308
	(2)	Mailed In-County Paid Subscriptions Stated on PS Form 3541 (Include paid distribution above nominal rate, advertiser's proof copies, and exchange copies)		
	(3)	Paid Distribution Outside the Mails Including Sales Through Dealers and Carriers, Street Vendors, Counter Sales, and Other Paid Distribution Outside USPS®	68	48
	(4)	Paid Distribution by Other Classes of Mail Through the USPS (e.g., First-Class Mail®)		
c. Total Paid Distribution (Sum of 15b (1), (2), (3), and (4)) ▶			530	356
d. Free or Nominal Rate Distribution (By Mail and Outside the Mail)	(1)	Free or Nominal Rate Outside-County Copies included on PS Form 3541		
	(2)	Free or Nominal Rate In-County Copies Included on PS Form 3541		
	(3)	Free or Nominal Rate Copies Mailed at Other Classes Through the USPS (e.g., First-Class Mail)		
	(4)	Free or Nominal Rate Distribution Outside the Mail (Carriers or other means)	2	2
e. Total Free or Nominal Rate Distribution (Sum of 15d (1), (2), (3) and (4))			2	2
f. Total Distribution (Sum of 15c and 15e) ▶			532	358
g. Copies not Distributed (See Instructions to Publishers #4 (page #3)) ▶			201	62
h. Total (Sum of 15f and g)			733	420
i. Percent Paid (15c divided by 15f times 100) ▶			99.62%	99.44%

* If you are claiming electronic copies, go to line 16 on page 3. If you are not claiming electronic copies, skip to line 17 on page 3.

PS Form 3526, July 2014 (Page 2 of 4)

UNITED STATES POSTAL SERVICE® Statement of Ownership, Management, and Circulation (All Periodicals Publications Except Requester Publications)

16. Electronic Copy Circulation	Average No. Copies Each Issue During Preceding 12 Months	No. Copies of Single Issue Published Nearest to Filing Date
a. Paid Electronic Copies ▶		
b. Total Paid Print Copies (Line 15c) + Paid Electronic Copies (Line 16a) ▶	530	356
c. Total Print Distribution (Line 15f) + Paid Electronic Copies (Line 16a) ▶	532	358
d. Percent Paid (Both Print & Electronic Copies) (16b divided by 16c × 100) ▶	99.62%	99.44%

☐ I certify that 50% of all my distributed copies (electronic and print) are paid above a nominal price.

17. Publication of Statement of Ownership
☒ If the publication is a general publication, publication of this statement is required. Will be printed in the December 2021 issue of this publication. ☐ Publication not required.

18. Signature and Title of Editor, Publisher, Business Manager, or Owner: LEON HAWKINS — Leon Hawkins, APA Circulation Manager — Date: 11/23/21

I certify that all information furnished on this form is true and complete. I understand that anyone who furnishes false or misleading information on this form or who omits material or information requested on the form may be subject to criminal sanctions (including fines and imprisonment) and/or civil sanctions (including civil penalties).

PS Form 3526, July 2014 (Page 3 of 4) PRIVACY NOTICE: See our privacy policy on www.usps.com.